2

AlGaN/GaN High Electron Mobility Transistor Based Sensors for Bio-Applications

Fan Ren[1], Stephen J. Pearton[2], Byoung Sam Kang[1] and Byung Hwan Chu[1]
[1]*Department of Chemical Engineering, University Florida*
[2]*Department of Materials Science and Engineering, University of Florida*
USA

1. Introduction

Chemical sensors have gained in importance in the past decade for applications that include homeland security, medical and environmental monitoring and also food safety. A desirable goal is the ability to simultaneously analyze a wide variety of environmental and biological gases and liquids in the field and to be able to selectively detect a target analyte with high specificity and sensitivity. In the area of detection of medical biomarkers, many different methods, including enzyme-linked immunsorbent assay (ELISA), particle-based flow cytometric assays, electrochemical measurements based on impedance and capacitance, electrical measurement of microcantilever resonant frequency change, and conductance measurement of semiconductor nanostructures. gas chromatography (GC), ion chromatography, high density peptide arrays, laser scanning quantitiative analysis, chemiluminescence, selected ion flow tube (SIFT), nanomechanical cantilevers, bead-based suspension microarrays, magnetic biosensors and mass spectrometry (MS) have been employed (Burlingame, Boyd and Gaskell 1996, Jackson and Chen 1996, Anderson, Bowden and Pickup 1996, Chen et al. 2003, Li et al. 2005, Zhang et al. 2006, Huber, Lang and Gerber 2008, Sandhu 2007, Zheng et al. 2005b). Depending on the sample condition, these methods may show variable results in terms of sensitivity for some applications and may not meet the requirements for a handheld biosensor.

For homeland security applications, reliable detection of biological agents in the field and in real time is challenging. During the anthrax attack on the World Bank in 2002, field tests showed 1200 workers to be positive, and all were sent home. 100 workers were provided antibiotics. However, confirmatory testing showed zero positives. False positives and false negatives can result due to very low volumes of samples available for testing and poor device sensitivities. Toxins such as ricin, botulinum toxin or enterotoxin B are environmentally stable, can be mass-produced and do not need advanced technologies for production and dispersal. The threat of these toxins is real. This is evident from the recent ricin detection from White House mail facilities and a US senator's office. Terrorists have already attempted to use botulinum toxin as a bio-weapon. Aerosols were dispersed at multiple sites in Tokyo, and at US military installations in Japan on at least 3 occasions between 1990 and 1995 by the Japanese cult Aum Shinrikyo (Greenfield et al. 2002). Four of the countries listed by the US government as "state sponsors of terrorism" (Iran, Iraq, North Korea, and Syria) (Greenfield et al. 2002) have developed, or are believed to be developing,

botulinum toxin as a weapon (Cordesman 1998, Bermudez 2001). After the 1991 Persian Gulf War, Iraq admitted to the United Nations inspection team to having produced 19000 L of concentrated botulinum toxin, of which approximately 10000 L were loaded into military weapons. This toxin has not been fully accounted for and constitutes approximately 3 times the amount needed to kill the entire current human population by inhalation (Greenfield et al. 2002). A significant issue is the absence of a definite diagnostic method and the difficulty in differential diagnosis from other pathogens that would slow the response in case of a terror attack. This is a critical need that has to be met to have an effective response to terrorist attacks. Given the adverse consequences of a lack of reliable biological agent sensing on national security, there is a critical need to develop novel, more sensitive and reliable technologies for biological detection in the field (Arnon et al. 2001). Some specific toxins of interest include Enterotoxin type B (Category B, NIAID), Botulinum toxin (Category A NIAID) and ricin (Category B NIAID).

While the techniques mentioned above show excellent performance under lab conditions, there is also a need for small, handheld sensors with wireless connectivity that have the capability for fast responses. The chemical sensor market represents the largest segment for sales of sensors, including chemical detection in gases and liquids, flue gas and fire detection, liquid quality sensors, biosensors and medical sensors. Some of the major applications in the home include indoor air quality and natural gas detection. Attention is now being paid to more demanding applications where a high degree of chemical specificity and selectivity is required. For biological and medical sensing applications, disease diagnosis by detecting specific biomarkers (functional or structural abnormal enzymes, low molecular weight proteins, or antigen) in blood, urine, saliva, or tissue samples has been established. Most of the techniques mentioned earlier such as ELISA possesses a major limitation in that only one analyte is measured at a time. Particle-based assays allow for multiple detection by using multiple beads but the whole detection process is generally longer than 2 hours, which is not practical for in-office or bedside detection. Electrochemical devices have attracted attention due to their low cost and simplicity, but significant improvements in their sensitivities are still needed for use with clinical samples. Microcantilevers are capable of detecting concentrations as low as 10 pg/ml, but suffer from an undesirable resonant frequency change due to the viscosity of the medium and cantilever damping in the solution environment. Nano-material devices have provided an excellent option toward fast, label-free, sensitive, selective, and multiple detections for both preclinical and clinical applications. Examples of detection of biomarkers using electrical measurements with semiconductor devices include carbon nanotubes for lupus erythematosus antigen detection (Chen et al. 2003), compound semiconducting nanowires and In_2O_3 nanowires for prostate-specific antigen detection (Li et al. 2005), and silicon nanowire arrays for detecting prostate-specific antigen [(Zheng et al. 2005a)]. In clinical settings, biomarkers for a particular disease state can be used to determine the presence of disease as well as its progress.

Semiconductor-based sensors can be fabricated using mature techniques from the Si chip industry and/or novel nanotechnology approaches. Silicon based sensors are still the dominant component of the semiconductor segment due to their low cost, reproducible and controllable electronic response. However, these sensors are not suited for operation in harsh environments, for instance, high temperature, high pressure or corrosive ambients. Si will be etched by some of the acidic or basic aqueous solutions encountered in biological sensing. By sharp contrast, GaN is not etched by any acid or base at temperatures below a

few hundred degrees. Therefore, wide band-gap group III nitride compound semiconductors (AlGaInN materials system) are alternative options to supplement silicon in these applications because of their chemical resistance, high temperature/high power capability, high electron saturation velocity and simple integration with existing GaN-based UV light-emitting diode, UV detectors and wireless communication chips.

A promising sensing technology utilizes AlGaN/GaN high electron mobility transistors (HEMTs). HEMT structures have been developed for use in microwave power amplifiers due to their high two dimensional electron gas (2DEG) mobility and saturation velocity. The conducting 2DEG channel of AlGaN/GaN HEMTs is very close to the surface and extremely sensitive to adsorption of analytes. HEMT sensors can be used for detecting gases, ions, pH values, proteins, and DNA.

The GaN materials system is attracting much interest for commercial applications of green, blue, and UV light emitting diodes (LEDs), laser diodes as well as high speed and high frequency power devices. Due to the wide-bandgap nature of the material, it is very thermally stable, and electronic devices can be operated at temperatures up to 500 °C. The GaN based materials are also chemically stable, and no known wet chemical etchant can etch these materials; this makes them very suitable for operation in chemically harsh environments. Due to the high electron mobility, GaN material based high electron mobility transistors (HEMTs) can operate at very high frequency with higher breakdown voltage, better thermal conductivity, and wider transmission bandwidths than Si or GaAs devices [(Makimoto, Yamauchi and Kumakura 2004, Zhang et al. 2003, Saito et al. 2006)].

An overlooked potential application of the GaN HEMT structure is sensors. The high electron sheet carrier concentration of nitride HEMTs is induced by piezoelectric polarization of the strained AlGaN layer in the hetero-junction structure of the AlGaN/GaN HEMT and the spontaneous polarization is very large in wurtzite III-nitrides. This provides an increased sensitivity relative to simple Schottky diodes fabricated on GaN layers or field effect transistors (FETs) fabricated on the AlGaN/GaN HEMT structure. The gate region of the HEMT can be used to modulate the drain current in the FET mode or use as the electrode for the Schottky diode. A variety of gas, chemical and health-related sensors based on HEMT technology have been demonstrated with proper surface functionalization on the gate area of the HEMTs, including the detection of hydrogen, mercury ion, prostate specific antigen (PSA), DNA, and glucose [(Jun et al. 2007, Yu et al. 2008, Wang et al. 2006a, Wang et al. 2007a, Anderson et al. 2008, Kim et al. 2003, Wang et al. 2005a, Schalwig et al. 2002, Luther, Wolter and Mohney 1999, Kang et al. 2005a, Wang et al. 2005b, Wright et al. 2009, Johnson et al. 2009, Lim et al. 2008, Tien et al. 2005a, Kryliouk et al. 2005, Tien et al. 2005b, Wang et al. 2005c, Eickhoff et al. 2003, Mehandru et al. 2004, Neuberger et al. 2001, Gangwani et al. 2007, Shen et al. 2004, Kang et al. 2007a, Kouche et al. 2005, Wang et al. 2007d, Kang et al. 2005d, Wang et al. 2007b, Chen et al. 2008, Pearton et al. 2007, Wang et al. 2007c, Kang et al. 2008, Kang et al. 2007d, Kang et al. 2004b, Lothian et al. 1992, Johnson et al. 2000, Kang et al. 2006, Kang et al. 2005c, Kang et al. 2007b, Kang et al. 2004a, Pearton et al. 2004)].

In this chapter, we discuss recent progress in the functionalization of these semiconductor sensors for applications in detection of pH measurement, biotoxins and other biologically important chemicals and the integration of these sensors into wireless packages for remote sensing capability.

2. Sensor functionalization

Specific and selective molecular functionalization of the semiconductor surface is necessary to achieve specificity in chemical and biological detection. Devices such as field effect transistors (FETs) can readily discriminate between adsorption of oxidizing and reducing gas molecules from the changes (increase or decrease) in the channel conductance. However, precise identification of a specific type of molecule requires functionalization of the surface with specific molecules or catalysts. Effective biosensing requires coupling of the unique functional properties of proteins, nucleic acids (DNA, RNA), and other biological molecules with the solid-state "chip" platforms. These devices take advantage of the specific, complementary interactions between biological molecules that are a fundamental aspect of biological function. Specific, complementary interactions are what permit antibodies to recognize antigens in the immune response, enzymes to recognize their target substrates, and the motor proteins of muscle to shorten during muscular contraction. The ability of biological molecules, such as proteins, to bind other molecules in a highly specific manner is the underlying principle of the "sensors" to detect the presence (or absence) of target molecules – just as it is in the biological senses of smell and taste.

One of the key technical challenges in fabricating hybrid biosensors is the junction between biological macromolecules and the inorganic scaffolding material (metals and semiconductors) of the chip. For actual device applications, it is often necessary to selectively modify a surface at micro- and even nano-scale, sometimes with different surface chemistry at different locations. In order to enhance detection speed, especially at very low analyte concentration, the analyte should be delivered directly to the active sensing areas of the sensors. A common theme for bio/chem sensors is that their operation often incorporates moving fluids. For example, sensors must sample a stream of air or water to interact with the specific molecules they are designed to detect.

The general approach to detecting biological species using a semiconductor sensor involves functionalizing the surface (e.g. the gate region of an ungated field effect transistor structure) with a layer or substance which will selectively bind the molecules of interest. In applications requiring less specific detection, the adsorption of reactive molecules will directly affect the surface charge and affect the near-surface conductivity. In their simplest form, the sensor consists of a semiconductor film patterned with surface electrodes and often heated to temperatures of a few hundred degrees Celsius to enhance dissociation of molecules on the exposed surface. Changes in resistance between the electrodes signal the adsorption of reactive molecules. It is desirable to be able to use the lowest possible operating temperature to maximize battery life in hand-held detection instruments. Electronic oxides such as ZnO as the sensing material are especially sensitive to reaction of target molecules with adsorbed oxygen or the oxygen in the lattice itself.

Biologically modified field effect transistors (bioFETs) have the potential to directly detect biochemical interactions in aqueous solutions. To enhance their practicality, the device must be sensitive to biochemical interactions on its surface, functionalized to probe specific biochemical interactions and must be stable in aqueous solutions for a range of pH and salt concentrations. Typically, the gate region of the device is covered with biological probes, which are used as receptor sites for the molecules of interest. The conductance of the device is changed as reaction occurs between these probes and appropriate species in solution.

Since GaN-based material systems are chemically stable, this should minimize degradation of adsorbed cells. The bond between Ga and N is ionic and proteins can easily attach to the

GaN surface. This is one of the key factors for making a sensitive biosensor with a useful lifetime. HEMT sensors have been used for detecting gases, ions, pH values, proteins, and DNA temperature with good selectivity by the modification of the surface in the gate region of the HEMT. The 2DEG channel is connected to an Ohmic-type source and drain contacts. The source-drain current is modulated by a third contact, a Schottky-type gate, on the top of the 2DEG channel. For sensing applications, the third contact is affected by the sensing environment, i.e. the sensing targets changes the charges on the gate region and behave as a gate. When charged analytes accumulate on the gate area, these charges form a bias and alter the 2DEG resistance. This electrical detection technique is simple, fast, and convenient. The detecting signal from the gate is amplified through the drain-source current and makes this sensor to be very sensitive for sensor applications. The electric signal also can be easily quantified, recorded and transmit, unlike fluorescence detection methods which need human inspection and are difficult to precisely quantify and transmit the data.

One drawback of HEMT sensors is a lack of selectivity to different analytes due to the chemical inertness of the HEMT surface. This can be solved by surface modification with detecting receptors. Sensor devices of the present disclosure can be used with a variety of fluids having environmental and bodily origins, including saliva, urine, blood, and breath. For use with exhaled breath, the device may include a HEMT bonded on a thermo-electric cooling device, which assists in condensing exhaled breath samples.

In our HEMT devices, the surface is generally functionalized with an antibody or enzyme layer. The success of the functionalization is monitored by a number of methods. Examples are shown in Figures 1 and 2. The first test is a change in surface tension when the functional layer is in place and the change in surface bonding can in some cases be seen by X-Ray Photoelectron Spectroscopy. Typically, a layer of Au is deposited on the gate region of the HEMT as a platform to attach a chemical such as thioglycolic acid, whose S-bonds readily attach to the Au. The antibody layer can then be attached to the thioglycolic acid. When the surface is completely covered by these functional layers, the HEMT will not be sensitive to buffer solutions or water that do not contain the antigen of interest, as shown in Figure 2. For detecting hydrogen, the gate region is functionalized with a catalyst metal such as Pt or Pd. In other cases, we immobilize an enzyme to catalyze reactions, as is used for the detection of glucose. In the presence of the enzyme glucose oxidase, glucose will react with oxygen to produce gluconic acid and hydrogen peroxide. Table I shows a summary of the surface functionalization layers we have employed for HEMT sensors to date. There are many additional options for detection of biotoxins and biological molecules of interest by use of different protein or antibody layers. The advantage of the biofet approach is that large arrays of HEMTs can be produced on a single chip and functionalized with different layers to allow for detection of a broad range of chemicals or gases.

3. pH Measurement

The measurement of pH is needed in many different applications, including medicine, biology, chemistry, food science, environmental science and oceanography. Solutions with a pH less than 7 are acidic and solutions with a pH greater than 7 are basic or alkaline. We have found that ZnO nanorod surfaces respond electrically to variations of the pH in electrolyte solutions introduced via an integrated microchannel [(Kang et al. 2005b)]. The ion-induced changes in surface potential are readily measured as a

change in conductance of the single ZnO nanorods and suggest that these structures are very promising for a wide variety of sensor applications. An integrated microchannel was made from SYLGARD@ 184 polymer. Entry and exit holes in the ends of the channel were made with a small puncher (diameter less than 1mm) and the film immediately applied to the nanorod sensor. The pH solution was applied using a syringe autopipette (2-20ul).

Detection	Mechanism	Surface Functionalization
H_2	Catalytic dissociation	Pd, Pt
Pressure change	polarization	Polyvinylidene difluoride
Botulinum toxin	antibody	Thioglycolic acid/antibody
Proteins	Conjugation/hybridization	Aminopropylsilane/biotin
pH	Adsorption of polar molecules	Sc_2O_3, ZnO
Hg^{2+}	chelation	Thioglycolic acid/Au
KIM-1	antibody	KIM-1 antibody
Glucose	GO_X immobilization	ZnO nanorods
Prostate Specific Antigen	PSA antibody	Carboxylate succimdyl ester/PSA antibody
Lactic acid	LO_X immobilization	ZnO nanorods
Chloride ions	Anodization	Ag/AgCl electrodes; InN
Breast Cancer	antibody	Thyioglycolic acid/c-erbB antibody
CO_2	Absorption of water/charge	Polyethylenimine/starch
DNA	hybridization	3′-thiol-modified oligonucleotides
O_2	oxidation	InGaZnO

Table 1. Summary of surface functional layers used with HEMT sensors

Prior to the pH measurements, we used pH 4, 7, 10 buffer solutions to calibrate the electrode and the measurements at 25 °C were carried out in the dark or under ultra-violet(UV) illumination from 365 nm light using an Agilent 4156C parameter analyzer to avoid parasitic effects. The pH solution made by the titration method using HNO_3, NaOH and distilled water. The electrode was a conventional Acumet standard Ag/AgCl electrode. The nanorods showed a very strong photoresponse. The conductivity is greatly increased as a result of the illumination, as evidenced by the higher current. No effect was observed for illumination with below bandgap light. The photoconduction appears predominantly to originate in bulk conduction processes with only a minor surface trapping component. The adsorption of polar molecules on the surface of ZnO affects the surface potential and device characteristics. The current at a bias of 0.5V as a function of time from nanorods exposed for 60s to a series of solutions whose pH was varied from 2-12 was reduced upon exposure to these polar liquids as the pH is increased. The experiment was conducted starting at pH=7 and went to pH=2 or 12. The I-V measurement in air was slightly higher that in the

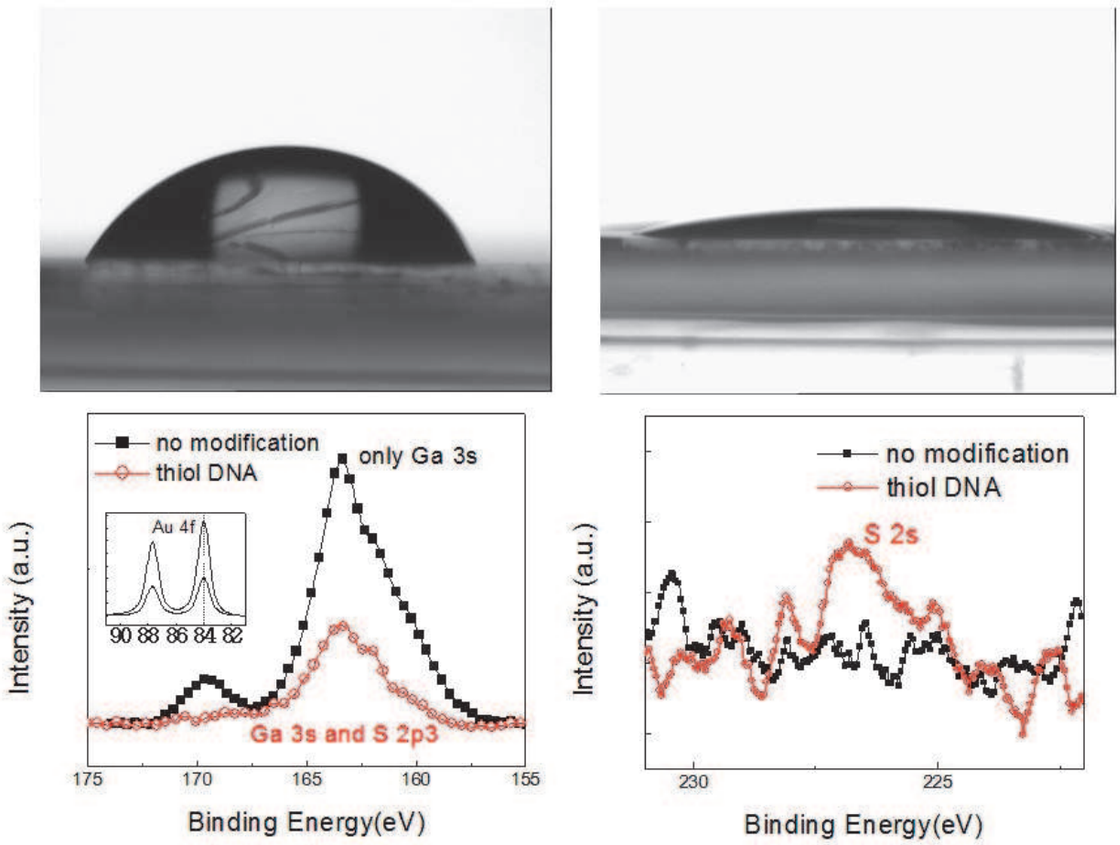

Fig. 1. Examples of a change in surface tension of the HEMT surface functionalization (top) and XPS measurement of formation of Au-S bonds after attachment of thioglycolic acid attachment to Au layer in gate region of HEMT.

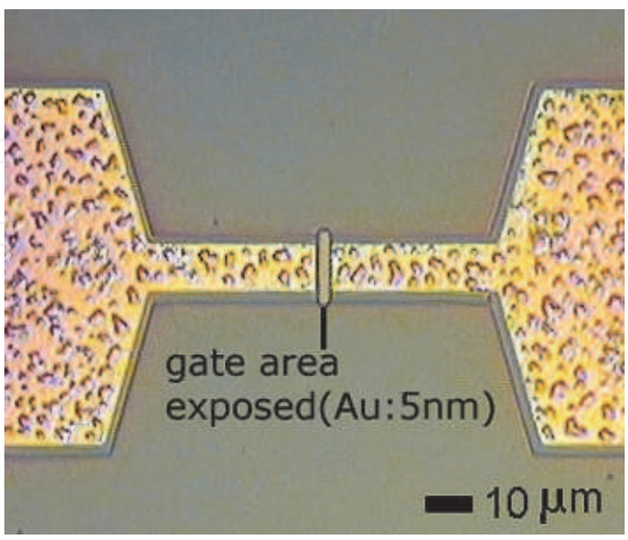

Fig. 2. Example of successful functionalization of HEMT surface-the device is no longer sensitive to water when the surface is completely covered with the functional layer.

pH=7(10-20%). The data in shows the sensor is sensitive to the concentration of the polar liquid and therefore could be used to differentiate between liquids into which a small amount of leakage of another substance has occurred. The conductance of the rods was higher under UV illumination but the percentage change in conductance is similar with and without illumination. The nanorods exhibited a linear change in conductance between pH 2-12 of 8.5nS/pH in the dark and 20nS/pH when illuminated with UV (365nm) light as shown at the bottom of Figure 16.The nanorods show stable operation with a resolution of ~0.1 pH over the entire pH range, showing the remarkable sensitivity to relatively small changes in concentration of the liquid.

Ungated AlGaN/ GaN HEMTs also exhibit large changes in current upon exposing the gate region to polar liquids. The polar nature of the electrolyte introduced led to a change of surface charges, producing a change in surface potential at the semiconductor /liquid interface. The use of Sc_2O_3 gate dielectric produced superior results to either a native oxide or UV ozone-induced oxide in the gate region. The ungated HEMTs with Sc_2O_3 in the gate region exhibited a linear change in current between pH 3-10 of 37μA/pH .The HEMT pH sensors show stable operation with a resolution of < 0.1 pH over the entire pH range. 100Å Sc_2O_3 was deposited as a gate dielectric through a contact window of SiN_x layer. Before oxide deposition, the wafer was exposed to ozone for 25 minutes. It was then heated in-situ at 300 °C cleaning for 10mins inside the growth chamber. The Sc_2O_3 was deposited by rf plasma-activated MBE at 100 °C using elemental Sc evaporated from a standard effusion at 1130 °C and O_2 derived from an Oxford RF plasma source. For comparison, we also fabricated devices with just the native oxide present in the gate region and also with the UV ozone -induced oxide. Figure 3 shows a scanning electron microscopy (SEM) image (top) and a cross-sectional schematic (bottom) of the completed device. The gate dimension of the device is 2 × 50 μm². The pH solution was applied using a syringe autopipette (2-20ul).

Prior to the pH measurements, we used pH 4, 7, 10 buffer solutions from Fisher Scientific to calibrate the electrode and the measurements at 25 °C were carried out in the dark using an Agilent 4156C parameter analyzer to avoid parasitic effects. The pH solution made by the titration method using HCl, NaOH and distilled water. The electrode was a conventional Acumet standard Ag/AgCl electrode.

The adsorption of polar molecules on the surface of the HEMT affected the surface potential and device characteristics. Figure 4 shows the current at a bias of 0.25V as a function of time from HEMTs with Sc_2O_3 in the gate region exposed for 150s to a series of solutions whose pH was varied from 3-10. The current is significantly increased upon exposure to these polar liquids as the pH is decreased. The change in current was 37 μA/pH.

The HEMTs show stable operation with a resolution of ~0.1 pH over the entire pH range, showing the remarkable sensitivity of the HEMT to relatively small changes in concentration of the liquid. By comparison, devices with the native oxide in the gate region showed a higher sensitivity of ~70 μA/pA but a much poorer resolution of ~0.4 pH and evidence of delays in response of 10-15 secs. The latter may result from deep traps at the interface between the semiconductor and native oxide, whose density is much higher than at the Sc_2O_3-nitride interface. The devices with UV-ozone oxide in the gate region did not show these incubation times for detection of pH changes and showed similar sensitivities of gate source current as the Sc_2O_3 gate devices (~40 μA/pH) but with poorer resolution (~0.25 pH). Figure 9 shows that the HEMT sensor with Sc_2O_3 gate dielectric is sensitive to the concentration of the polar liquid and therefore could be used to differentiate between

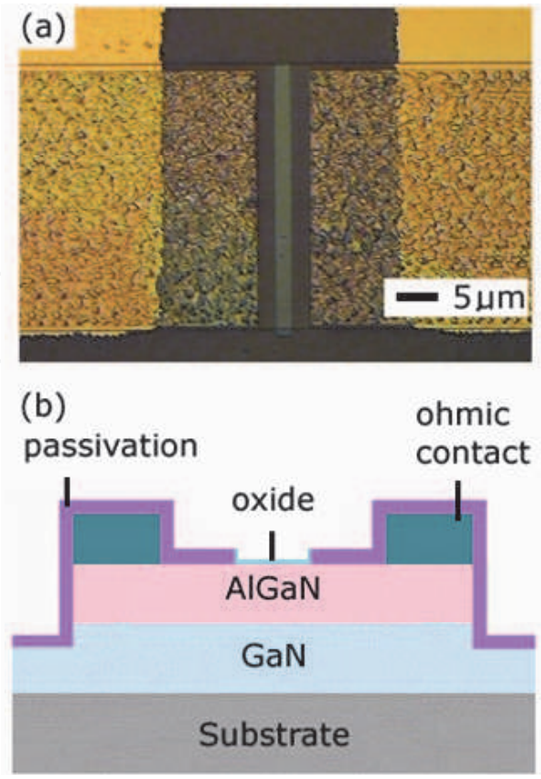

Fig. 3. (a) SEM and schematic of gateless HEMT. (b) Schematic of the pH sensor.

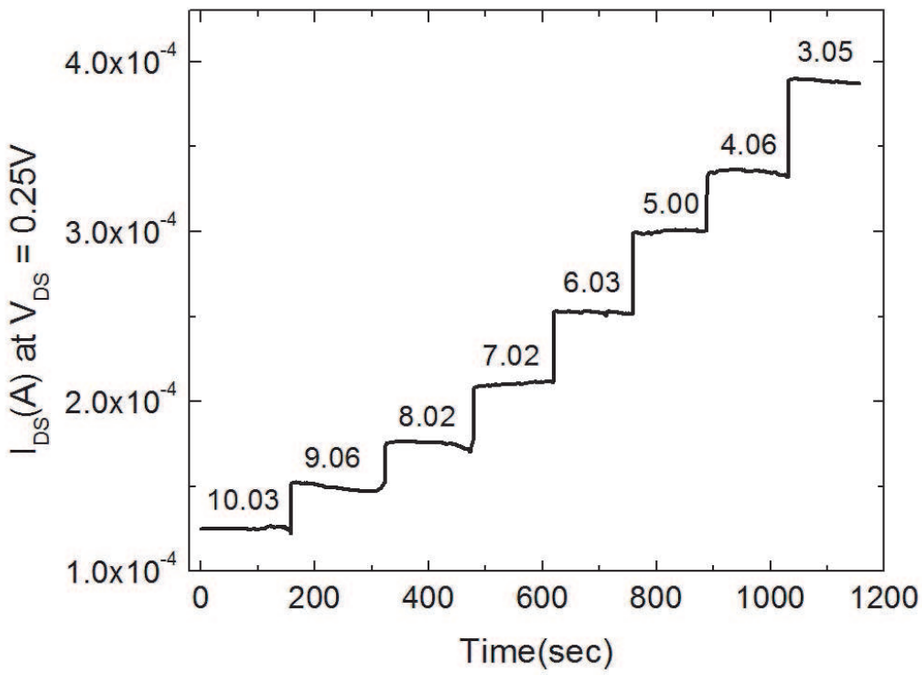

Fig. 4. Change in current in gateless HEMT at fixed source-drain bias of 0.25 V with pH from 3-10.

liquids into which a small amount of leakage of another substance has occurred. As mentioned earlier, the pH range of interest for human blood is 7-8. Figure 5 shows the current change in the HEMTs with Sc_2O_3 at a bias of 0.25V for different pH values in this range. Note that the resolution of the measurement is < 0.1 pH. There is still more to understand about the mechanism of the current reduction in relation to the adsorption of the polar liquid molecules on the HEMT surface. These molecules are bonded by van der-Waals type interactions and they screen surface change that is induced by polarization in the HEMT.

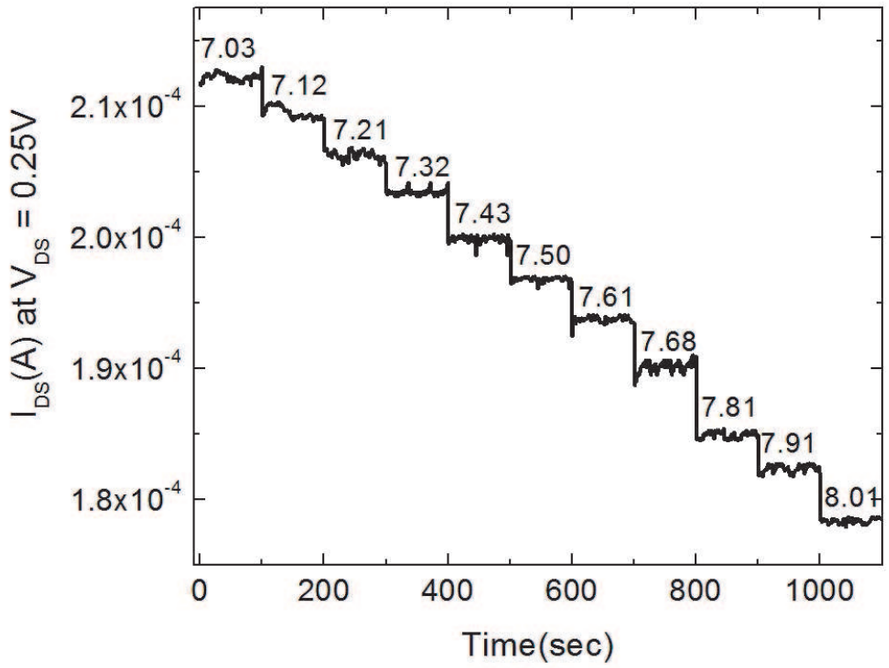

Fig. 5. Change in current in gateless HEMT at fixed source-drain bias of 0.25 V with pH from 7-8.

4. Sensing the pH value in the exhaled breath condensate

There is significant interest in developing rapid diagnostic approaches and improved sensors for determining early signs of medical problems in humans. Exhaled breath is a unique bodily fluid that can be utilized in this regard (Horvath et al. 2005, Namjou, Roller and McCann 2006, Machado et al. 2005, Kullmann et al. 2007, Vaughan et al. 2003, Hunt et al. 2000, Kostikas et al. 2002, Carpagnano et al. 2005, Gessner et al. 2003, Kullmann et al. 2008, Accordino et al. 2008, Czebe et al. 2008). Exhaled breath condensate pH is a robust and reproducible assay of airway acidity. For example, the blood pH range that is relevant for humans is 7-8. Humans, even when they are extremely ill, will not have a blood (or interstitial = space between cells in tissue) pH below 7. When they do drift below this value, it almost invariably equals mortality.

While most applications will detect substances or diseases in the breath as a gas or aerosol, breath can also be analyzed in the liquid phase as exhaled breath condensate (EBC). Analytes contained in the breath originating from deep within the lungs (alveolar gas)

equilibrates with the blood, and therefore the concentration of molecules present in the breath is closely correlated with those found in the blood at any given time. EBC contains dozens of different biomarkers, such as adenosine, ammonia, hydrogen peroxide, isoprostanes, leukotrienes, peptide, cytokines and nitrogen oxide (Kullmann et al. 2008, Accordino et al. 2008, Czebe et al. 2008). Analysis of molecules in EBC is noninvasive and can provide a window on the metabolic state of the human body, including certain signs of cancer, respiratory diseases, liver and kidney functions.

As a diagnostic, exhaled breath offers advantages since samples can be collected and tested with results delivered in real time at the point of testing. Another advantage is that the sample can be collected non-invasively by asking a patient to blow into the disposable portion of a handheld testing device. Therefore, the sample collection method is hygienic for both the patient and the laboratory personnel. Exhaled breath can be used to detect various drugs, medications, their metabolites and markers, and this can be valuable in measuring both medication adherence and in determining the blood levels of these drugs and medications. Some of today's blood and urine-based tests might be replaced with simple breath-based testing. In consumer healthcare, diabetics would be able to test their glucose level, replacing painful and inconvenient finger-prick devices. For roadside screening of driving impairment, a point-of-care (POC) device similar in function to a handheld breath alcohol analyzer will detect drugs of abuse such as marijuana and cocaine. In workplace drug testing, a similar desktop device might eliminate the cost, embarrassment and inconvenience of workplace urine screening. In the setting of chronic oral drug therapy (e.g., treatment of schizophrenia with atypical antipsychotic medications), mortality/morbidity and the cost of health care will be markedly reduced by developing breath-based systems that document that drugs were orally ingested and entered the blood stream.

The glucose oxidase enzyme (GOx) is commonly used in biosensors to detect levels of glucose for diabetics. By keeping track of the number of electrons passed through the enzyme, the concentration of glucose can be measured. Due to the importance and difficulty of glucose immobilization, numerous studies have been focused on the techniques of immobilization of glucose with carbon nanotubes, ZnO nano-materials, and gold particles (Bloemen et al. 2007, Park, Boo and Chung 2006). ZnO-based nano-materials are especially interesting due to their non-toxic properties, low cost of fabrication and favorable electrostatic interaction between ZnO and the GOx lever. However, the activity of GOx is highly dependent on the pH value of the solution (Pandey et al. 2007). The pH value of a typical healthy person is between 7 and 8. This can vary significantly depending on the health condition of each individual, e.g. the pH value for patients with acute asthma was reported as low as 5.23 + 0.21 (n=22) as compared to 7.65 + 0.20 (n=19) for the control subjects (Kouassi, Irudayaraj and McCarty 2005). To achieve accurate glucose concentration measurement with immobilized GO_x, it is necessary to determine the pH value and glucose concentration with an integrated pH and glucose sensor.

AlGaN/GaN HEMTs can be used for measurements of pH in EBC and glucose, through integration of the pH and glucose sensor onto a single chip and with additional integration of the sensors into a portable, wireless package for remote monitoring applications. Figure 6 shows an optical microscopy image of an integrated pH and glucose sensor chip and cross-sectional schematics of the completed pH and glucose device. The gate dimension of the pH sensor device and glucose sensors was 20 × 50 μm^2.

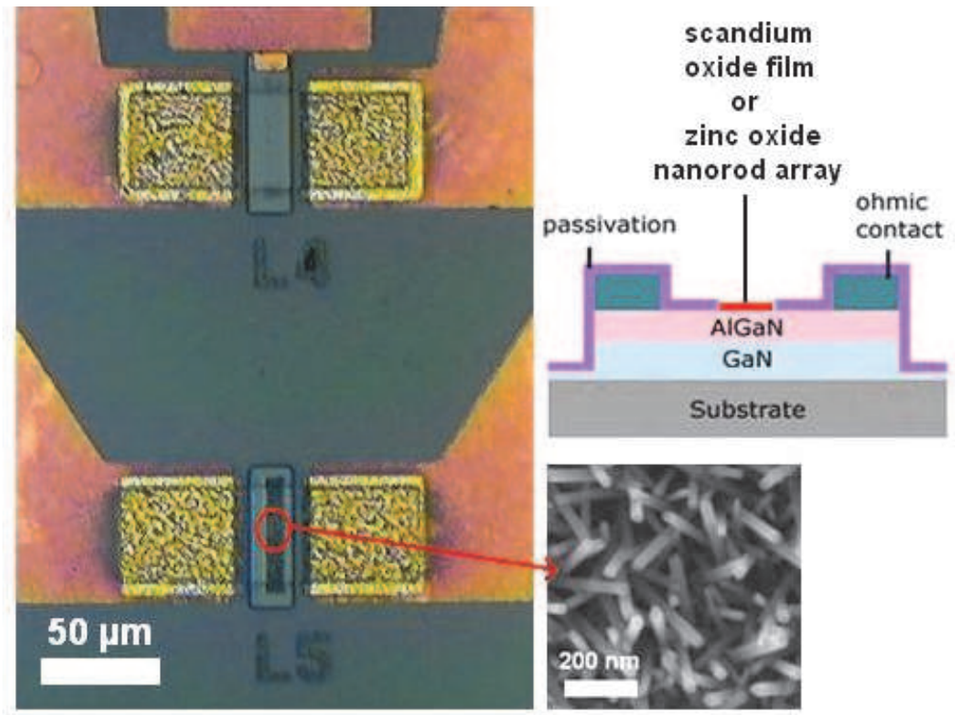

Fig. 6. SEM image of an integrated pH and glucose sensor. The insets show a schematic cross-section of the pH sensor and also an SEM of the ZnO nanorods grown in the gate region of the glucose sensor.

For the glucose detection, a highly dense array of 20-30 nm diameter and 2 µm tall ZnO nanorods were grown on the 20 × 50 µm² gate area. The lower right inset in Figure 6 shows closer view of the ZnO nanorod arrays grown on the gate area. The total area of the ZnO was increased significantly with the ZnO nanorods. The ZnO nanorod matrix provides a microenvironment for immobilizing negatively charged GO_x while retaining its bioactivity, and passes charges produced during the GO_x and glucose interaction to the AlGaN/GaN HEMT. The GOx solution was prepared with concentration of 10 mg/mL in 10 mM phosphate buffer saline (pH value of 7.4, Sigma Aldrich). After fabricating the device, 5 µl GO_x (~100 U/mg, Sigma Aldrich) solution was precisely introduced to the surface of the HEMT using a pico-liter plotter. The sensor chip was kept at 4 °C in the solution for 48 hours for GO_x immobilization on the ZnO nanorod arrays followed by an extensively washing to remove the un-immobilized GO_x.

To take the advantage of quick response (less than 1 sec) of the HEMT sensor, a real-time EBC collector is needed (Montuschi and Barnes 2002, Anh, Olthuis and Bergveld 2005). The amount of the EBC required to cover the HEMT sensing area is very small. Each tidal breath contains around 3 l of the EBC. The contact angle of EBC on Sc_2O_3 has been measured to be less than 45°, and it is reasonable to assume a perfect half sphere of EBC droplet formed to cover the sensing area 4 × 50 µm² gate area. The volume of a half sphere with a diameter of 50 µm is around 3×10^{-11} liter. Therefore, 100,000 of 50 µm diameter droplets of EBC can be formed from each tidal breath. To condense entire 3 l of water vapor, only ~ 7 J of energy need to be removed for each tidal breath, which can be easily achieved with a thermal electric module, a Peltier device, as shown in Figure 7. The

schematic of the system for collecting the EBC is illustrated in Figure 8. The AlGaN/GaN HEMT sensor is directly mounted on the top of the Peltier unit (TB-8-0.45-1.3 HT 232, Kryotherm), as also shown in Figure 7, which can be cooled to precise temperatures by applying known voltages and currents to the unit. During our measurements, the hotter plate of the Peltier unit was kept at 21°C, and the colder plate was kept at 7 °C by applying bias of 0.7 V at 0.2 A. The sensor takes less than 2 sec to reach thermal equilibrium with the Peltier unit. This allows the exhaled breath to immediately condense on the gate region of the HEMT sensor.

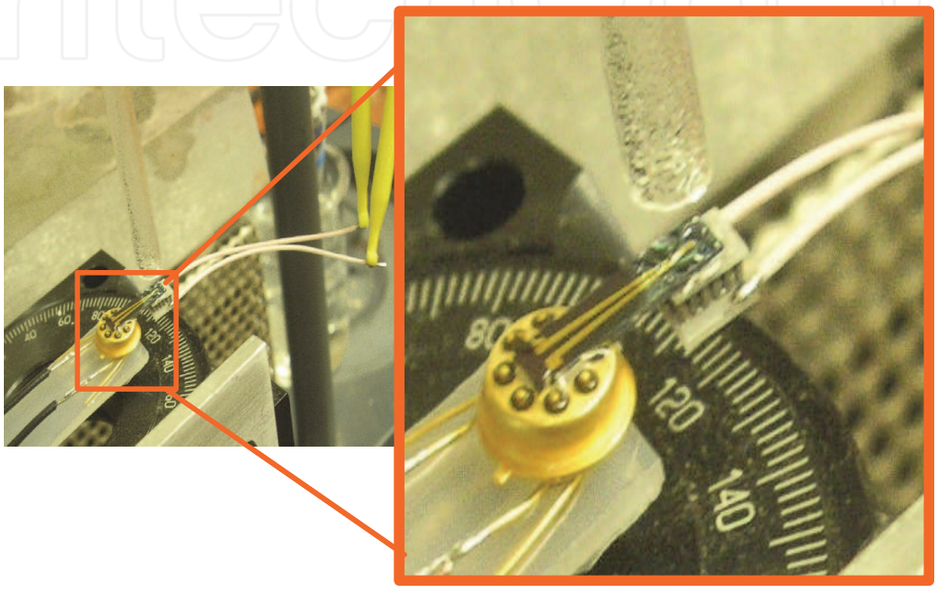

Fig. 7. Optical image of sensor mounted on Peltier cooler.

Prior to pH measurements of the EBC, a Hewlett Packard soap film flow meter and a mass flow controller were used to calibrate the flow rate of exhaled breath. The HEMT sensors were also calibrated and exhibited a linear change in current between pH 3-10 of 37μA/pH. Due to the difficulty to collect the EBC with different glucose concentration, the samples for glucose concentration detection were prepare from glucose diluted in PBS or DI water.

The HEMT sensors were not sensitive to switching of N_2 gas, but responded to applications of exhaled breath pulse inputs from a human test subject, as shown at the top of Figure 9 (top), which shows the current of a Sc_2O_3 capped HEMT sensor biased at 0.5V for exposure to different flow rates of exhaled breath (0.5-3.0 l/min). The flow rates are directly proportional to the intensity exhalation. Deep breath provides a higher flow rate. A similar study was conducted with pure N_2 to eliminate the flow rate effect on sensor sensitivity. The N_2 did not cause any change of drain current, but the increase of exhaled breath flow rate decreased the drain current proportionally from 0.5 L/min to a saturation value of 1 L/min. For every tidal breath, the beginning portion of the exhalation is from the physiologic dead space, and the gases in this space do not participate in CO_2 and O_2 exchange in the lungs. Therefore, the contents in the tidal breath are diluted by the gases from this dead space. For higher flow rate exhalation, this dilution effect is less effective. Once the exhaled breath flow rate is above 1L/min, the sensor current change reaches a limit. As a result, the test subject experiences hyper ventilation and the dilution becomes insignificant. Figure 9 (bottom) shows the time response of the sensors to much longer exhaled breaths.

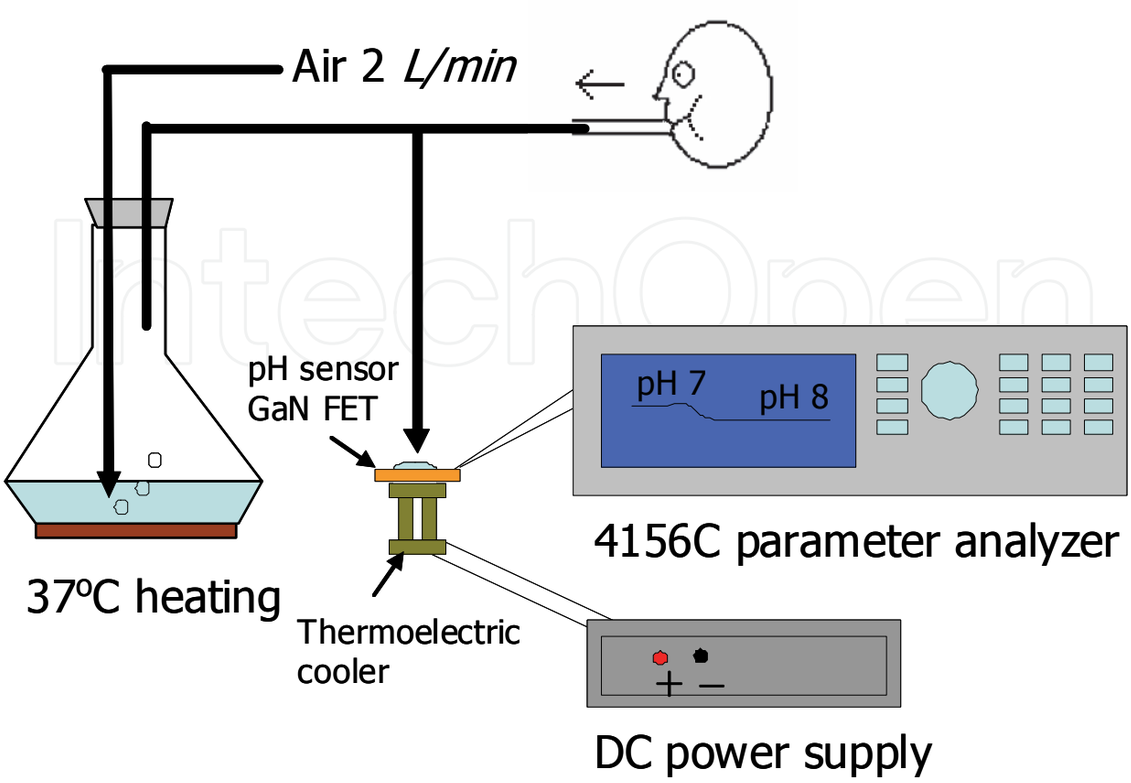

Fig. 8. Schematic of the system for collecting EBC.

The characteristic shape of the response curves is similar and is determined by the evaporation of the condensed EBC from the gate region of the HEMT sensor. The sensor is operated at 50 Hz and 10% duty cycle, which produces heat during operation. It only takes a few seconds for the EBC to vaporize from the sensing area and causes the spike-like response. The principal component of the EBC is water vapor, which represents nearly all of the volume (>99%) of the fluid collected in the EBC. The measured current change of the exhale breath condensate shows that the pH values are within the range between pH 7 and 8. This range is the typical pH range of human blood.

5. Glouse sensing

The glucose was sensed by ZnO nanorod functionalized HEMTs with glucose oxidase enzyme localized on the nanorods, shown in Figure 10. This catalyzes the reaction of glucose and oxygen to form gluconic acid and hydrogen peroxide. Figure 11 shows the real time glucose detection in PBS buffer solution using the drain current change in the HEMT sensor with constant bias of 250 mV. No current change can be seen with the addition of buffer solution at around 200 sec, showing the specificity and stability of the device. By sharp contrast, the current change showed a rapid response of less than 5 seconds when target glucose was added to the surface. So far, the glucose detection using Au nano-particle, ZnO nanorod and nanocomb, or carbon nanotube material with GOx immobilization is based on electrochemical measurement (Wang et al. 2006b, Wei et al. 2006, Yang et al. 2004, Hrapovic et al. 2004).

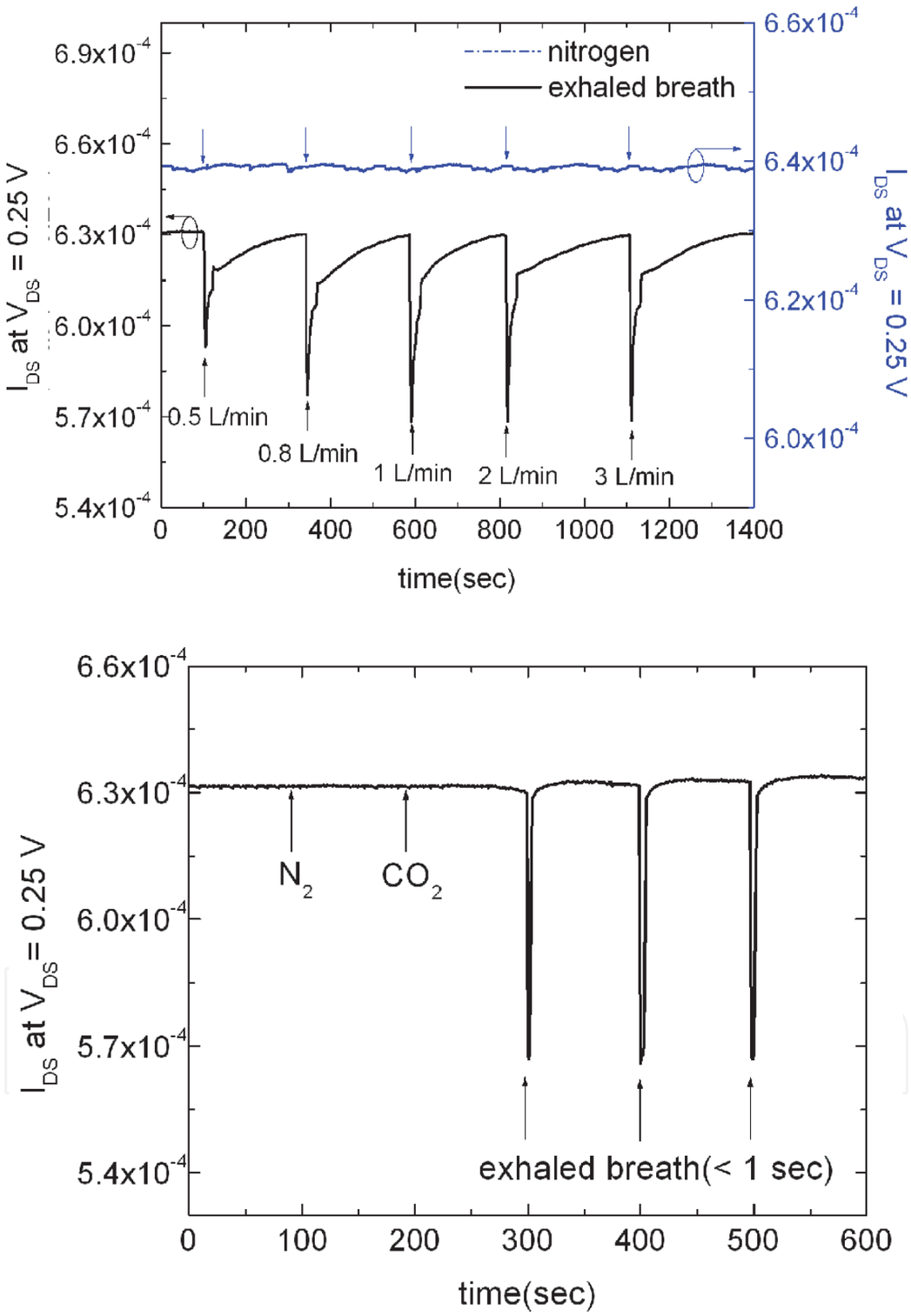

Fig. 9. Changes of drain current for HEMT sensor at fixed drain-source bias of 0.5 V with different flow rates or durations of exhaled breath from tidal breath to hyperventilation .The duration of the breath is 5 secs in the bottom figure.

Since there is a reference electrode required in the solution, the volume of sample can not be easily minimized. The current density is measured when a fixed potential applied between nano-materials and the reference electrode. This is a first order detection and the range of detection limit of these sensors is 0.5-70 μM. Even though the AlGaN/GaN HEMT based sensor used the same GOx immobilization, the ZnO nanorods were used as the gate of the HEMT. The glucose sensing was measured through the drain current of HEMT with a change of the charges on the ZnO nano-rods and the detection signal was amplified through the HEMT. Although the response of the HEMT based sensor is similar to that of an electrochemical based sensor, a much lower detection limit of 0.5 nM was achieved for the HEMT based sensor due to this amplification effect. Since there is no reference electrode required for the HEMT based sensor, the amount of sample only depends on the area of gate dimension and can be minimized. The sensors do not respond to glucose unless the enzyme is present, as shown in Figure 12.

Although measuring the glucose in the EBC is a noninvasive and convenient method for the diabetic application, the activity of the immobilized GO_x is highly dependent on the pH value of the solution. The GOx activity can be reduced to 80% for pH = 5 to 6. If the pH value of the glucose solution is larger than 8, the activity drops off very quickly (Kouassi et al. 2005). Figure 31 shows the time dependent source-drain current signals with constant drain bias of 500 mV for glucose detection in DI water and PBS buffer solution. 50 l of PBS solution was introduced on the glucose sensor and no current change can be seen with the addition of buffer solution at 20 and 30 min. This stability is important to exclude possible noise from the mechanical change of the buffer solution. By sharp contrast, the current change showed a rapid response in less than 20 seconds when the sensor was dipped into the 100 ml of 10 mM glucose solution using DI water as the solvent. This sudden drain current increase indicated that GOx immediately reacted with glucose and oxygen was produced as a by-production of this reaction. However, the drain current gradually decreased. This was due to the oxygen produced in the GOx-glucose interaction reacting with water and changing the pH value adjacent the gate area. Since there was not agitation in the glucose solution, the solution around gate area became more basic and the activity of GOx decreased due to the high pH value environment from 60 to 85 min.

Because the lower activity of GOx in the high pH value condition, the amount of oxygen produced from GOx and glucose decreased as well during the period of 60-85 min. Once the OH^- ions produce from reaction between oxygen and water diffused away the gate area, the pH value decreased. Thus around 85 min, the pH value of the glucose solution around gate area decreased low enough to allow the activity of GOx to resume and the drain current of the glucose sensor showed another sudden increase. Then, the same process happened again and drain current of the glucose current gradually decreased for a second time.

On the contrary, when the glucose sensor was used in a pH controlled environment, the drain current stayed fairly constant, as shown in Figure 13. In this experiment, 50 l of PBS solution was introduced on the glucose sensor to establish the base line of the sensor as in the previous experiment. Then, glucose of 10 nM concentration prepared in PBS solution was introduced to the gate area of the glucose sensor through a micro-injector. There was no glucose in the 50 l PBS solution and the PBS solution was added at 20 and 30 min. It took time for the glucose solution to diffuse to the gate area of the sensor through the blank PBS and the drain current gradually increased corresponding to the glucose diffusion process. Since the fresh glucose was continuously provided to the sensor surface and the

pH value of the glucose was controlled, once the concentration of the glucose reached equilibrium at the gate of the glucose sensor, the drain current of the glucose remained constant except in the presence of glucose solution, which was taken out from time to time using a micro-pipette. There were small oscillations of the drain current observed, which could be eliminated by using a microfluidic device for this experiment.

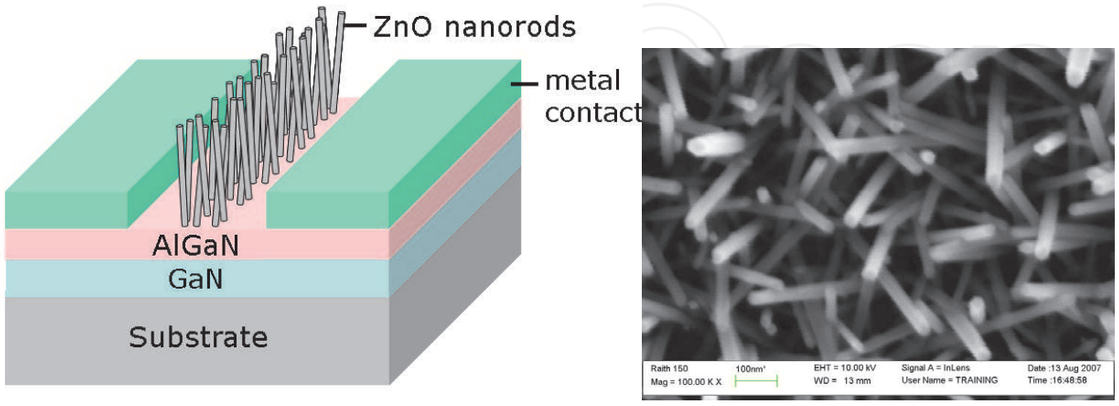

Fig. 10. (left) Schematic of ZnO nanorod functionalized HEMT and (right) SEM of nanorods on gate area.

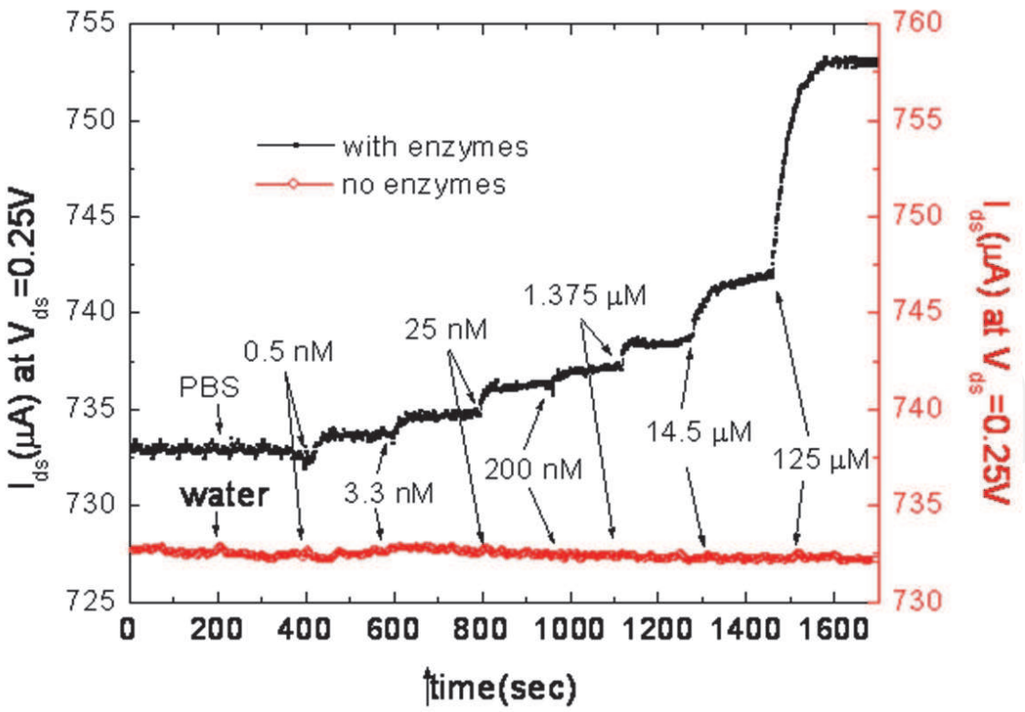

Fig. 11. Plot of drain current versus time with successive exposure of glucose from 500 pM to 125 M in 10 mM phosphate buffer saline with a pH value of 7.4, both with and without the enzyme located on the nanorods.

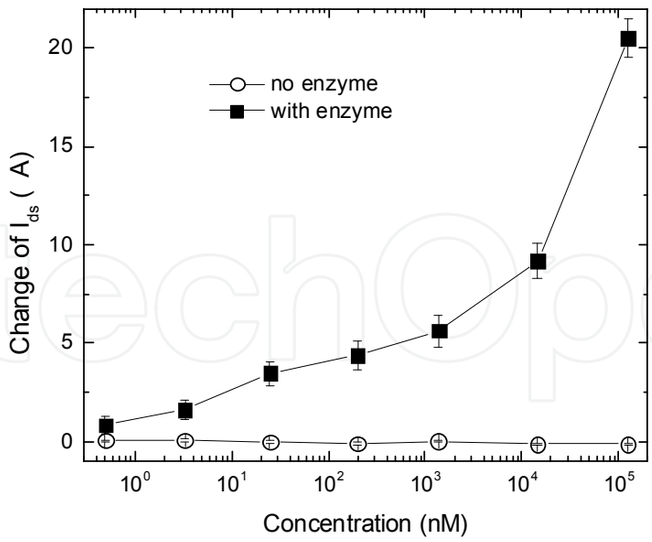

Fig. 12. Change in drain-source current in HEMT glucose sensors both with and without localized enzyme.

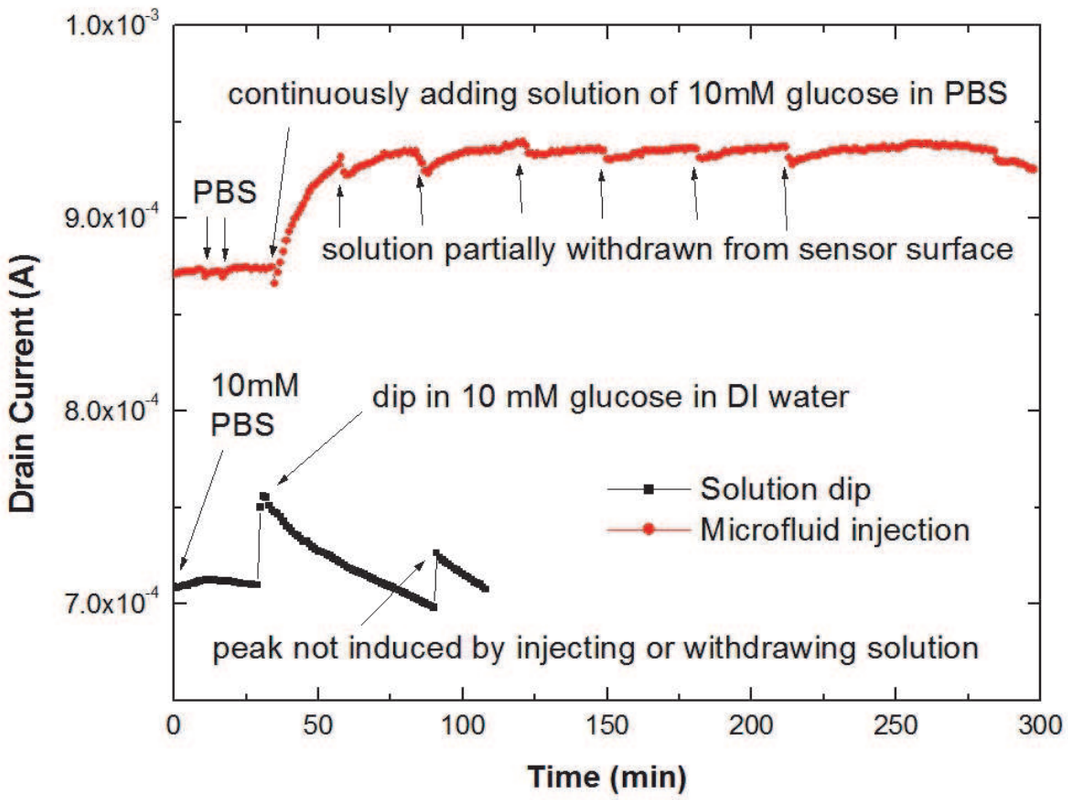

Fig. 13. Plot of drain current versus time by dipping the glucose sensor in 10 mM of glucose dissolved in DI water (black line) and exposing the sensor to continuously flow of 10 mM of glucose dissolved in phosphate buffer saline with a pH value of 7.4(red line).

The human pH value can vary significantly depending on the health condition. Since we cannot control the pH value of the EBC samples, we needed to measure the pH value while determine the glucose concentration in the EBC. With the fast response time and low volume of the EBC required for HEMT based sensor, a handheld and real-time glucose sensing technology can be realized.

6. Bio-toxin sensing

Reliable detection of biological agents in the field and in real time is challenging. Given the adverse consequences of a lack of reliable biological agent sensing on national security, there is a critical need to develop novel, more sensitive and reliable technologies for biological detection in the field (Arnon et al. 2001, Greenfield et al. 2002, Michaelson, Halpern and Kopans 1999, Harrison et al. 1998, McIntyre et al. 1999, Bigler et al. 2002, Paige and Streckfus 2007, Streckfus et al. 1999, Streckfus et al. 2000b, Streckfus et al. 2000a, Streckfus et al. 2001, Streckfus and Bigler 2005, Streckfus, Bigler and Zwick 2006, Chase 2000, Navarro et al. 1997, Bagramyan et al. 2008). The objective of this application is to develop and test a wireless sensing technology for detecting logicalb toxins. To achieve this objective, we have developed high electron mobility transistors (HEMTs) that have been demonstrated to exhibit some of the highest sensitivities for biological agents. Specific antibodies targeting Enterotoxin type B (Category B, NIAID), Botulinum toxin (Category A NIAID) and ricin (Category B NIAID), or peptide substrates for testing the toxin's enzymatic activity, have been conjugated to the HEMT surface. While testing still needs to be performed in the presence of cross-contaminants in biologically relevant samples, the initial results are very promising. A significant issue is the absence of a definite diagnostic method and the difficulty in differential diagnosis from other pathogens that would slow the response in case of a terror attack. Our aim is to develop reliable, inexpensive, highly sensitive, hand-held sensors with response times on the order of a few seconds, which can be used in the field for detecting biological toxins. This is significant because it would greatly improve our effectiveness in responding to terrorist attacks.

The current methods for toxin sensing in the field are generally not suited for field deployment and there is a need for new technologies. The current methods involve the use of HPLC, mass spectrometry and colorimetric ELISAs which are impractical because such tests can only be carried out at centralized locations, and are too slow to be of practical value in the field. These still tend to be the methods of choice in current detection of toxins, e.g. the standard test for botulinum toxin detection is the 'mouse assay', which relies on the death of mice as an indicator of toxin presence (Bagramyan et al. 2008). Clearly, such methods are slow and impractical in the field.

Antibody-functionalized Au-gated AlGaN/GaN high electron mobility transistors (HEMTs) show great sensitivity for detecting botulinum toxin. The botulinum toxin was specifically recognized through botulinum antibody, anchored to the gate area, as shown in Figure 14.

We investigated a range of concentrations from 0.1 ng/ml to 100 ng/ml. The source and drain current from the HEMT were measured before and after the sensor was exposed to 100 ng/ml of botulinum toxin at a constant drain bias voltage of 500 mV, as shown in Figure 16 (top). Any slight changes in the ambient of the HEMT affect the surface charges on the AlGaN/GaN. These changes in the surface charge are transduced into a change in the concentration of the 2DEG in the AlGaN/GaN HEMTs, leading to the decrease in the conductance for the device after exposure to botulinum toxin.

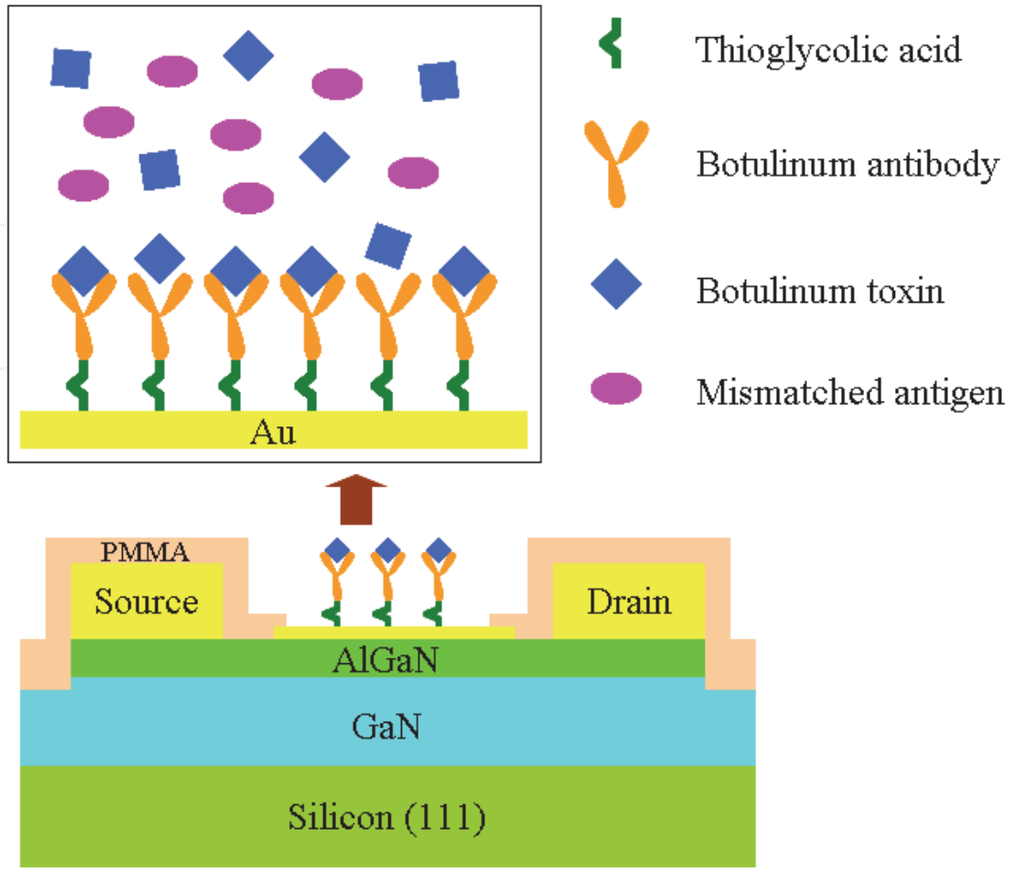

Fig. 14. Schematic of functionalized HEMT for botulinum detection.

Figure 16 (bottom) shows a real time botulinum toxin detection in PBS buffer solution using the source and drain current change with constant bias of 500 mV. No current change can be seen with the addition of buffer solution around 100 seconds, showing the specificity and stability of the device. In clear contrast, the current change showed a rapid response in less than 5 seconds when target 1 ng/ml botulinum toxin was added to the surface. The abrupt current change due to the exposure of botulinum toxin in a buffer solution was stabilized after the botulinum toxin thoroughly diffused into the buffer solution. Different concentrations (from 0.1 ng/ml to 100 ng/ml) of the exposed target botulinum toxin in a buffer solution were detected. The sensor saturates above 10ng/ml of the toxin. The experiment at each concentration was repeated four times to calculate the standard deviation of source-drain current response. The limit of detection of this device was below 1 ng/ml of botulinum toxin in PBS buffer solution. The source-drain current change was nonlinearly proportional to botulinum toxin concentration, as shown in Figure 15.

Figure 16 shows a real time test of botulinum toxin at different toxin concentrations with intervening washes to break antibody-antigen bonds. This result demonstrates the real-time capabilities and recyclability of the chip. Long term stability of the botulinum toxin sensor was also investigated with a package sensor. Figure 17 shows a photograph of the packaged sensor placed in a Petri dish for long term storage. PBS buffer solution was dropped on the active region of the sensor and the Petri dish as well. The Petri dish was then covered and sealed in order to keep the antibodies on the sensor in a PBS environment.

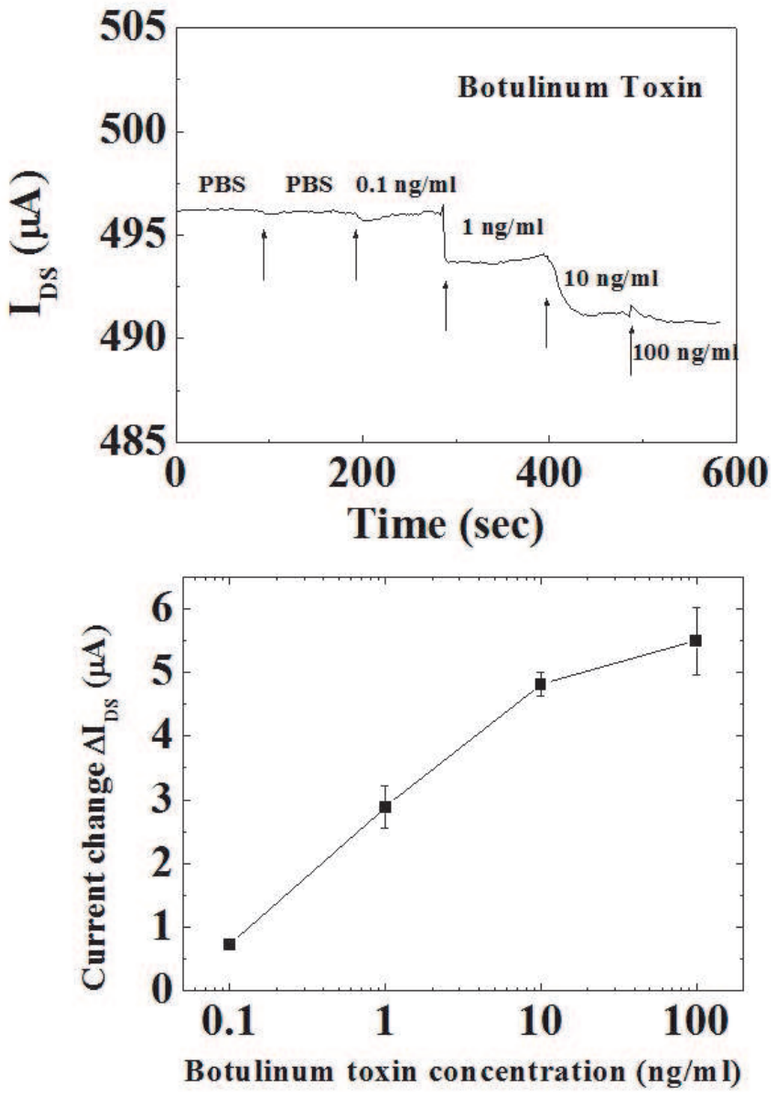

Fig. 15. Drain current of an AlGaN/GaN HEMT versus time for botulinum toxin from 0.1 ng/ml to 100 ng/ml(top) and change of drain current versus different concentrations from 0.1 ng/ml to 100 ng/ml of botulinum toxin (bottom).

Sensors were re-tested for the botulinum detection every three months. For those tests, the procedures of toxin detection and sensor surface reactivation were repeated for five times. This experiment demonstrated that after 9 month storage, the sensor still could detect the toxin and could be reactivated right after the test with PBS buffer solution rinse. This indicated that the toxin could be completely washed away from the antibodies. However, it was obvious that the detection sensitivity decreased after 9 months of storage. The decrease of the detection sensitivity drop after 9 month storage was not caused by the existence of the un-breakable toxin-antibody binding, but was rather due to the decrease of antibody activity. Another important finding was that the response time of the 9 month stored sensor increased from 5 seconds of the fresh sensor to around 10 seconds, when target toxins were exposed to the sensor. The longer response time may be also due to the decreased number of

highly active sites on the antibodies after long term storage. This corresponds to the lower sensitivity of the sensor. The detailed mechanism needs further investigation.

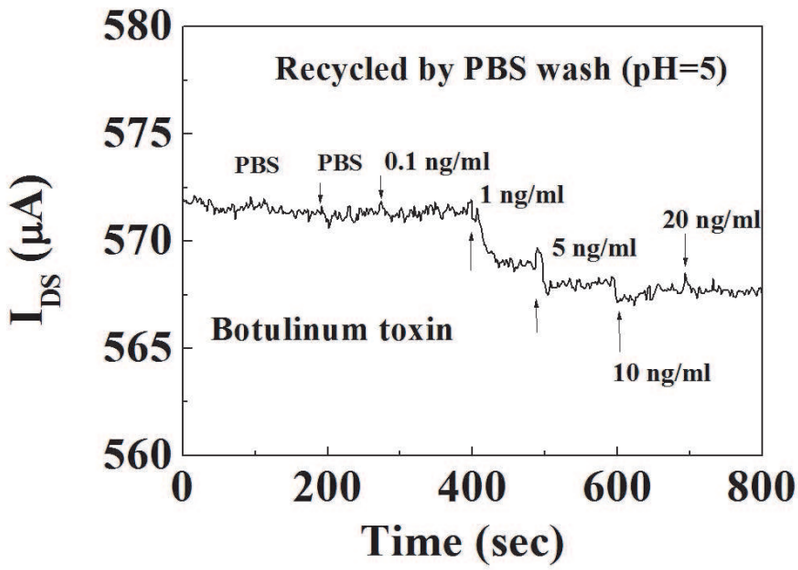

Fig. 16. Real-time test from a used botulinum sensor which was washed with PBS in pH 5 to refresh the sensor.

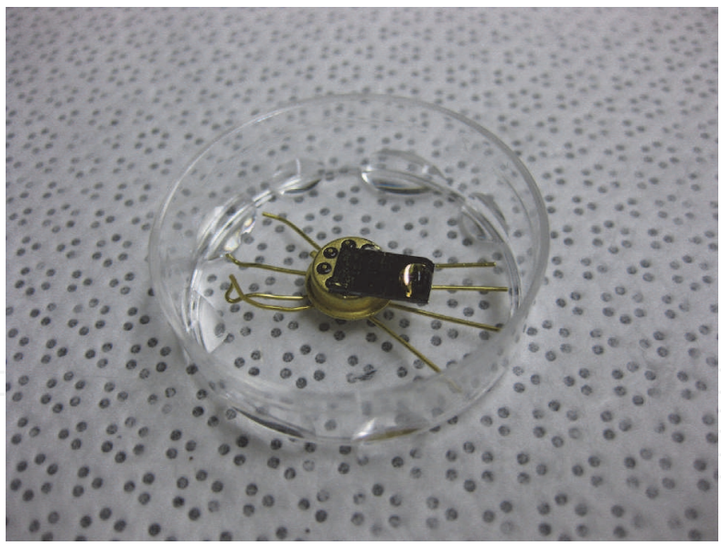

Fig. 17. Photograph of a packaged sensor placed in a Petri dish for long term storage.

Figure 18 shows the current changes of the sensors tested after different storage times at a fixed toxin concentration of 10 ng/ml against the first drain current measurement of the sensor. After 3, 6 and 9 months of storage, the current change drops 2%, 12% and 28%, respectively. Within 3 months of storage, this sensor showed almost the same sensitivity as when it was fresh. Although, after 6 and 9 months of storage, the sensor would need to be re-calibrated for toxin concentration determination usage, there is no need for recalibration for the use as the first responder of the detection for the presence or absence of the toxin.

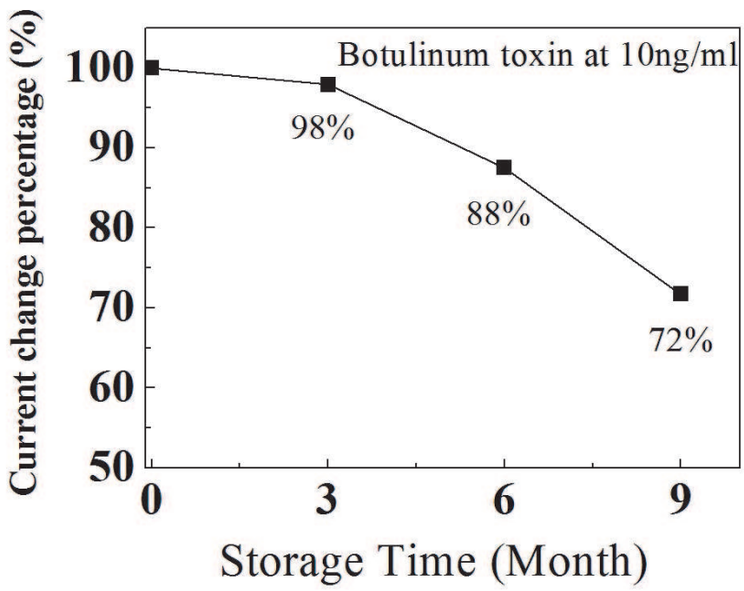

Fig. 18. The drain-source current change percentages of the initial, 3, 6 and 9 month stored sensors. The current change in the initial test is defined as 100%. The testing at the subsequent periods was defined relative to the initial test.

In summary, we have shown that through a chemical modification method, the Au-gated region of an AlGaN/GaN HEMT structure can be functionalized for the detection of botulinum toxin with a limit of detection less than 1 ng/ml. This electronic detection of biomolecules is a significant step towards a field-deployed sensor chip, which can be integrated with a commercial available wireless transmitter to realize a real-time, fast response and high sensitivity botulinum toxin detector.

7. Biomedical applications

7.1 Prostate cancer detection

Prostate cancer is the second most common cause of cancer death among men in the United States (Kelloff et al. 2004). The most commonly used serum marker for diagnosis of prostate cancer is prostate specific antigen (PSA) (Thompson and Ankerst 2007, Healy et al. 2007). The market size for prostate cancer testing is enormous. According to the American Cancer Society, prostate cancer is the most common form of cancer among men, other than skin cancer. It is estimated that during 2007, in the United States alone, 218,890 new cases of prostate cancer will be diagnosed and 1 in 6 men will be diagnosed with prostate cancer during his lifetime .

The American Cancer Society recommends health care professionals to offer the prostate-specific antigen (PSA) blood test and the digital rectal exam (DRE) yearly for men above the age of 50. Those men who have a higher risk, such as African Americans and men who have a first-degree relative diagnosed with prostate cancer should start testing at 45. Men who have several first-degree relatives diagnosed with prostate cancer should begin testing at 40. Since 1990, a recent awareness of cancers and the benefits of early detection have increased

early detection tests for prostate cancer and they have grown to become fairly common. Prostate cancer can often be found early by testing the amount of prostate-specific antigen (PSA) in the patient's blood. It can also be detected on a digital rectal exam (DRE). If you have routine yearly exams and either one of these test results becomes abnormal, then any cancer you might have has likely been found at an early, more treatable stage.

The prostate cancer testing market is expected to grow over the upcoming years. As awareness of cancer and early detection increases, so too will the need for testing. Given the high demand for prostate cancer testing, one would think that there are many options for early detection. However, there are only two main ways for preliminary testing for prostate cancer: the prostate cancer antigen blood test and the digital rectal exam. Prostate-specific antigen (PSA) is made by cells in the prostate gland and although PSA is mostly found in semen, a certain amount is found in the blood as well. Most men have PSA levels under 4 nanograms per milliliter of blood. When prostate cancer develops, the PSA level usually goes up above 4 nanograms per milliliter; however, about 15% of men with a PSA below 4 will have prostate cancer on biopsy. If the patient's PSA level is between 4 and 10, their chance of having prostate cancer is about 25%. If the patient's PSA level is above 10, there is more than a 50% chance they have prostate cancer, which increases as the PSA level goes up. If the patient's PSA level is high, the doctor may advise a prostate biopsy to find out if they have cancer.

Generally PSA testing approaches are costly, time-consuming and need sample transportation. A number of different electrical measurements have been used for rapid detection of PSA(Wang 2006, Fernández-Sánchez et al. 2004, Hwang et al. 2004, Wee et al. 2005, Wang et al. 2009, Anderson et al. 2009). For example, electrochemical measurements based on impedance and capacitance are simple and inexpensive but need improved sensitivities for use with clinical samples (Wang 2006, Fernández-Sánchez et al. 2004). Resonant frequency changes of an anti-PSA antibody coated microcantilever enable a detection sensitivity of ~ 10 pg/ml but this micro-balance approach has issues with the effect of the solution on resonant frequency and cantilever damping (Fernández-Sánchez et al. 2004, Hwang et al. 2004). Antibody-functionalized nanowire FETs coated with antibody provide for low detection levels of PSA (Wang et al. 2009, Anderson et al. 2009), but the scale-up potential is limited by the expensive e-beam lithography requirements. Antibody functionalized Au-gated AlGaN/GaN HEMTs shown schematically in Figure 19 were found to be effective for detecting PSA at low concentration levels.

The PSA antibody was anchored to the gate area through the formation of carboxylate succinimdyl ester bonds with immobilized thioglycolic acid. The HEMT drain-source current showed a response time of less than 5 seconds when target PSA in a buffer at clinical concentrations was added to the antibody-immobilized surface. The devices could detect a range of concentrations from 1 μg/ml to 10 pg/ml. The lowest detectable concentration was two orders of magnitude lower than the cut-off value of PSA measurements for clinical detection of prostate cancer. Figure 20 shows the real time PSA detection in PBS buffer solution using the source and drain current change with constant bias of 0.5V(Kang et al. 2007c). No current change can be seen with the addition of buffer solution or nonspecific bovine serum albumin (BSA), but there was a rapid change when10 ng/ml PSA was added to the surface. The abrupt current change due to the exposure of PSA in a buffer solution could be stabilized after the PSA diffused into the buffer solution. The ultimate detection limit appears to be a few pg/ml (Kang et al. 2007c).

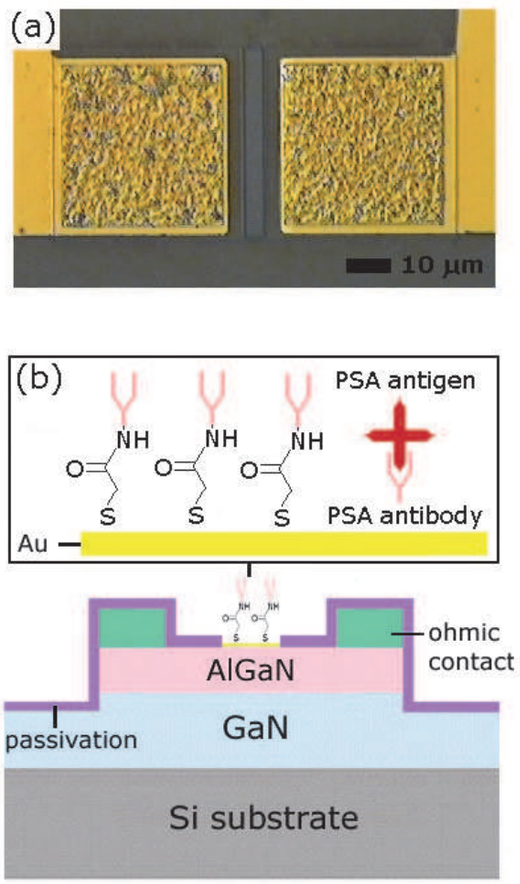

Fig. 19. Schematic of HEMT sensor functionalized for PSA detection.

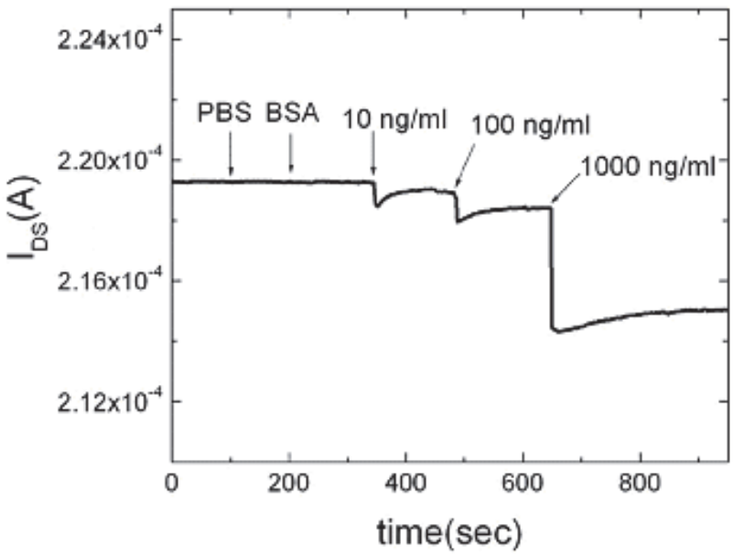

Fig. 20. Drain current versus time for PSA detection when sequentially exposed to PBS, BSA, and PSA

7.2 Kidney injury molecule detection

Problems such as Acute Kidney Injury (AKI) or Acute Renal Failure (ARF) are unfortunately still associated with a high mortality rate (Thadhani, Pascual and Bonventre 1996, Chertow et al. 1998, Bonventre and Weinberg 2003). An important biomarker for early detection of AKI is the urinary antigen known as kidney injury molecule-1 or KIM-1(Ichimura et al. 1998) and this is generally carried out with the ELISA technique discussed earlier (Vaidya and Bonventre 2006, Vaidya et al. 2006, Lequin 2005). The biomarker can also be detected with particle-based flow cytometric assay, but the cycle time is several hours (Vignali 2000). Electrical measurement approaches based on carbon nanotubes (Chen et al. 2003), nanowires of In_2O_3 (Li et al. 2005) or Si (Zheng et al. 2005b, Patolsky, Zheng and Lieber 2006a, Patolsky, Zheng and Lieber 2006b, Patolsky et al. 2007, Han et al. 2005), or Si or GaN FETs look promising for fast and sensitive detection of anibodies and potentially for molecules such as KIM-1(Thadhani et al. 1996, Chertow et al. 1998, Bonventre and Weinberg 2003, Ichimura et al. 1998, Vaidya and Bonventre 2006, Vaidya et al. 2006, Lequin 2005, Vignali 2000, Chen et al. 2003, Li et al. 2005, Zheng et al. 2005b, Patolsky et al. 2006a, Patolsky et al. 2006b, Patolsky et al. 2007, Han et al. 2005).

The functionalization scheme in the gate region began with thioglycolic acid followed by KIM-1 antibody coating (Wang et al. 2007d). The gate region was deposited with a 5 nm thick Au film. Then the Au was conjugated to specific KIM-1 antibodies with a self-assembled monolayer of thioglycolic acid. The HEMT source-drain current showed a clear dependence on the KIM-1 concentration in phosphate-buffered saline (PBS) buffer solution, as shown in Figure 21 where the time dependent source-drain current at a bias of 0.5 V is plotted for KIM-1 detection in PBS buffer solution. The limit of detection (LOD) was 1ng/ml using a 20 μm ×50 μm gate sensing area (Wang et al. 2007d).

7.3 Breast cancer detection

The market size for breast cancer testing is vast – nearly 200,000 women and 1,700 men were diagnosed in 2006 alone. Although lucrative, competition in this industry is strong. Growth potential is possible, however, as the most effective and widely used diagnostic exam for breast cancer, the mammogram, is potentially harmful due to radiation exposure. Other, less popular, exams that do not involve radiation tend to be both invasive and expensive. Currently, the overwhelming majority of patients are screened for breast cancer by mammography . This procedure involves a high cost to the patient and is invasive (radiation) which limits the frequency of screening. Breast cancer is currently the most common female malignancy in the world, representing 7% of the more than 7.6 million cancer-related deaths worldwide. Breast cancer accounts for over 30% of all new diagnoses in women aged 20-49 and 50-69, and 20% among older women. As a result, more than one million mammograms are performed each year. According to the National Breast Cancer Foundation, it is estimated that nearly 200,000 women and 1,700 men will be diagnosed with breast cancer this year.

When breast cancer is discovered early on, there is a much better chance of successful treatment. Therefore it is highly recommended that women check their breasts monthly from the age of 20. Clinical breast examinations should be conducted every three years from ages 20-39 and an annual mammogram for women 50 and older. Work by Michaelson et al. (Michaelson et al. 1999) indicates a 96% survival rate if patients could be screened every three months. Thus, mortality in breast cancer patients could be reduced by increasing the frequency of screening. However this is not feasible presently due to the lack of cheap and reliable technologies that can screen breast cancer non-invasively.

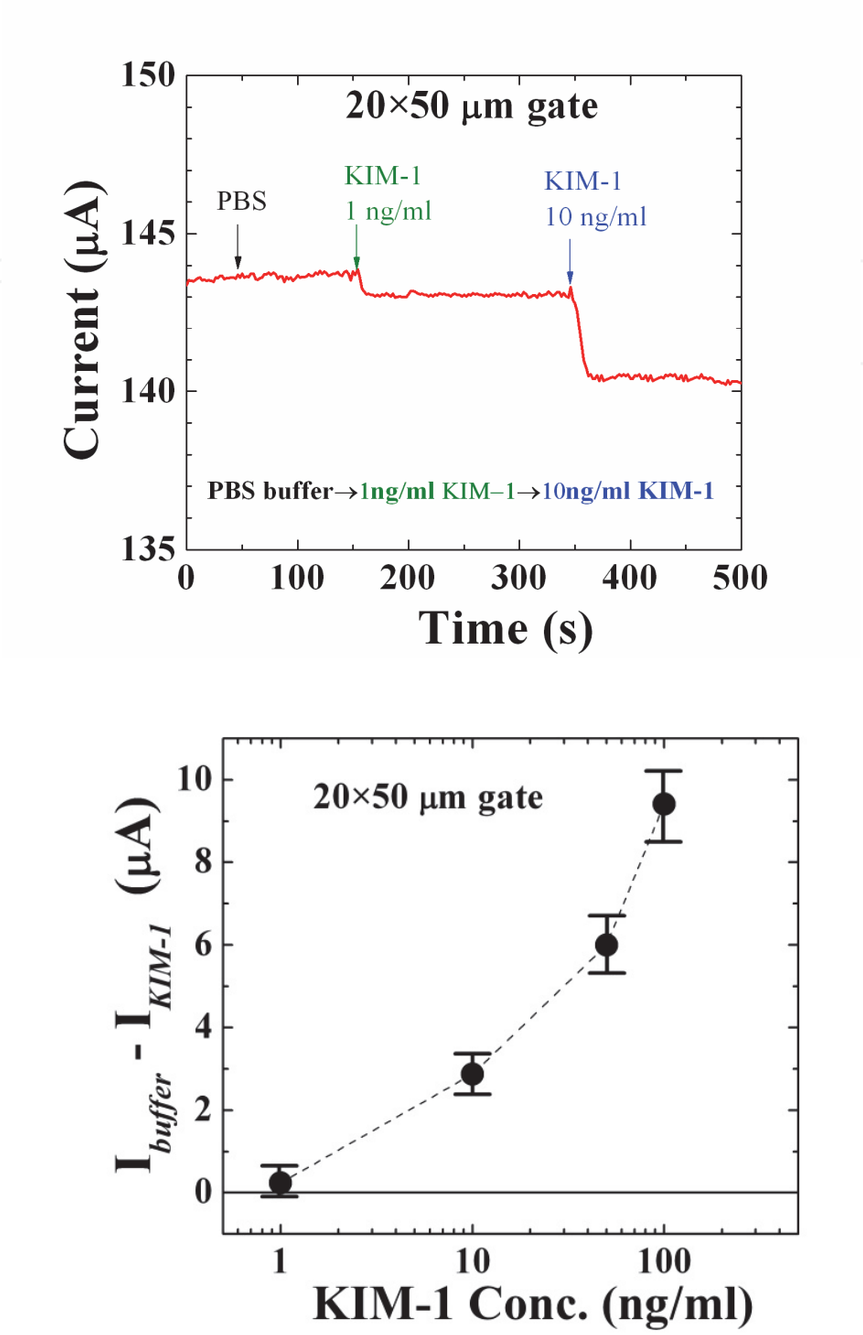

Fig. 21. Time dependent current signal when exposing the HEMT to 1ng/ml and 10ng/ml KIM-1 in PBS buffer.

There is recent evidence to suggest that salivary testing for makers of breast cancer may be used in conjunction with mammography (Bigler et al. 2002, Harrison et al. 1998, McIntyre et al. 1999, Streckfus et al. 1999, Streckfus et al. 2000b, Streckfus et al. 2000a, Streckfus et al. 2001, Streckfus and Bigler 2005, Streckfus et al. 2006, Chase 2000). Saliva-based diagnostics for the protein c-erbB-2, have tremendous prognostic potential (Streckfus and Bigler 2005,

Paige and Streckfus 2007). Soluble fragments of the c-erbB-2 oncoprotein and the cancer antigen 15-3 were found to be significantly higher in the saliva of women who had breast cancer than in those patients with benign tumors (Streckfus et al. 2006). Other studies have shown that epidermal growth factor (EGF) is a promising marker in saliva for breast cancer detection (Paige and Streckfus 2007, Navarro et al. 1997). These initial studies indicate that the saliva test is both sensitive and reliable and can be potentially useful in initial detection and follow-up screening for breast cancer. However, to fully realize the potential of salivary biomarkers, technologies are needed that will enable facile, sensitive, specific detection of breast cancer.

Antibody-functionalized Au-gated AlGaN/GaN high electron mobility transistors (HEMTs) show promise for detecting c-erbB-2 antigen. The c-erbB-2 antigen was specifically recognized through c-erbB antibody, anchored to the gate area. We investigated a range of clinically relevant concentrations from 16.7 μg/ml to 0.25 μg/ml.

The Au surface was functionalized with a specific bi-functional molecule, thioglycolic acid. We anchored a self-assembled monolayer of thioglycolic acid, $HSCH_2COOH$, an organic compound and containing both a thiol (mercaptan) and a carboxylic acid functional group, on the Au surface in the gate area through strong interaction between gold and the thiol-group of the thioglycolic acid. The devices were first placed in the ozone/UV chamber and then submerged in 1 mM aqueous solution of thioglycolic acid at room temperature. This resulted in binding of the thioglycolic acid to the Au surface in the gate area with the COOH groups available for further chemical linking of other functional groups. The device was incubated in a phosphate buffered saline (PBS) solution of 500 μg/ml c-erbB-2 monoclonal antibody for 18 hours before real time measurement of c-erbB-2 antigen.

After incubation with a PBS buffered solution containing c-erbB-2 antibody at a concentration of 1 μg/ml, the device surface was thoroughly rinsed off with deionized water and dried by a nitrogen blower. The source and drain current from the HEMT were measured before and after the sensor was exposed to 0.25 μg/ml of c-erbB-2 antigen at a constant drain bias voltage of 500 mV. Any slight changes in the ambient of the HEMT affect the surface charges on the AlGaN/GaN. These changes in the surface charge are transduced into a change in the concentration of the 2DEG in the AlGaN/GaN HEMTs, leading to the slight decrease in the conductance for the device after exposure to c-erbB-2 antigen.

Figure 22 shows real time c-erbB-2 antigen detection in PBS buffer solution using the source and drain current change with constant bias of 500 mV. No current change can be seen with the addition of buffer solution around 50 seconds, showing the specificity and stability of the device. In clear contrast, the current change showed a rapid response in less than 5 seconds when target 0.25 μg/ml c-erbB-2 antigen was added to the surface. The abrupt current change due to the exposure of c-erbB-2 antigen in a buffer solution was stabilized after the c-erbB-2 antigen thoroughly diffused into the buffer solution. Three different concentrations (from 0.25 μg/ml to 16.7 μg/ml) of the exposed target c-erbB-2 antigen in a buffer solution were detected. The experiment at each concentration was repeated five times to calculate the standard deviation of source-drain current response.

The limit of detection of this device was 0.25 μg/ml c-erbB-2 antigen in PBS buffer solution. The source-drain current change was nonlinearly proportional to c-erbB-2 antigen concentration, as shown in Figure 23. Between each test, the device was rinsed with a wash buffer of 10 mM, pH 6.0 phosphate buffer solution containing 10 mM KCl to strip the antibody from the antigen.

Clinically relevant concentrations of the c-erbB-2 antigen in the saliva and serum of normal patients are 4-6 µg/ml and 60-90 µg/ml respectively. For breast cancer patients, the c-erbB-2 antigen concentrations in the saliva and serum are 9-13 µg/ml and 140-210 µg/ml, respectively. Our detection limit suggests that HEMTs can be easily used for detection of clinically relevant concentrations of biomarkers. Similar methods can be used for detecting other important disease biomarkers and a compact disease diagnosis array can be realized for multiplex disease analysis.

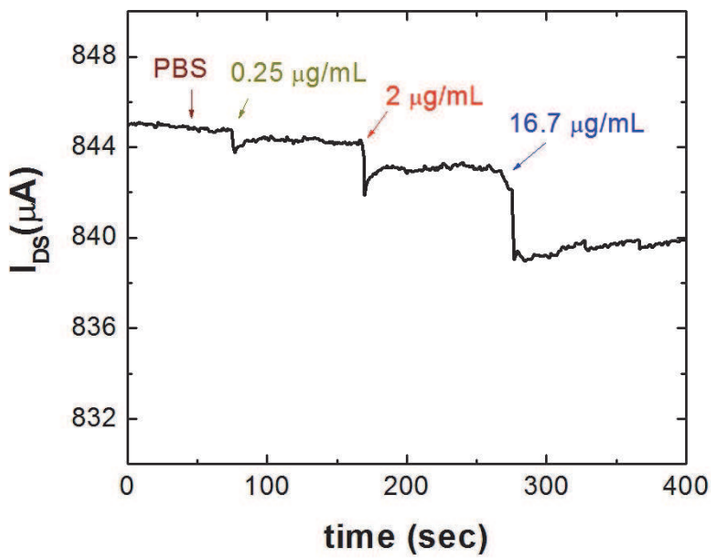

Fig. 22. Drain current of an AlGaN/GaN HEMT over time for c-erbB-2 antigen from 0.25 µg/ml to 17 µg/ml.

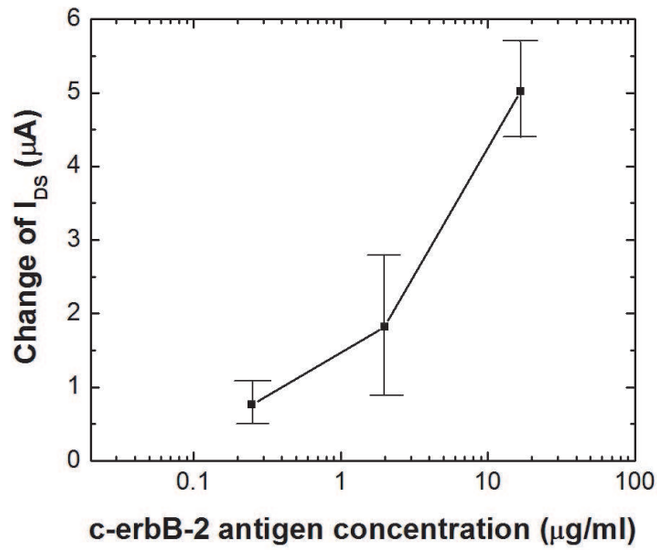

Fig. 23. Drain current as a function of c-erbB-2 antigen concentrations from 0.25 µg/ml to 17 µg/ml.

7.4 Lactic acid detection

Lactic acid can also be detected with ZnO nanorod-gated AlGaN/GaN HEMTs. Interest in developing improved methods for detecting lactate acid has been increasing due to its importance in areas such as clinical diagnostics, sports medicine, and food analysis. An accurate measurement of the concentration of lactate acid in blood is critical to patients that are in intensive care or undergoing surgical operations as abnormal concentrations may lead to shock, metabolic disorder, respiratory insufficiency, and heart failure. Lactate acid concentration can also be used to monitor the physical condition of athletes or of patients with chronic diseases such as diabetes and chronic renal failure. In the food industry, lactate level can serve as an indicator of the freshness, stability and storage quality. For the reasons above, it is desirable to develop a sensor capable of simple and direct measurements, rapid response, high specificity, and low cost. Recent researches on lactate acid detection mainly focus on amperometric sensors with lactate acid specific enzymes attached to an electrode with a mediator (Parra et al. 2006, Phypers and Pierce 2006, Lin, Shih and Chau 2007, Spohn et al. 1996, Pohanka and Zboril 2008, Suman et al. 2005, Haccoun et al. 2006, Di et al. 2007). Examples of materials used as mediators include carbon paste, conducting copolymer, nanostructured Si_3N_4 and silica materials. Other methods of detecting lactate acid include utilizing semiconductors (Lupu et al. 2007) and electro-chemiluminescent materials (Marquette, Degiuli and Blum 2000).

A ZnO nanorod array, which was used to immobilize lactate oxidase oxidase (LOx), was selectively grown on the gate area using low temperature hydrothermal decomposition as illustrated in Figure 24. The array of one-dimensional ZnO nanorods provided a large effective surface area with high surface-to-volume ratio and a favorable environment for the immobilization of LOx.

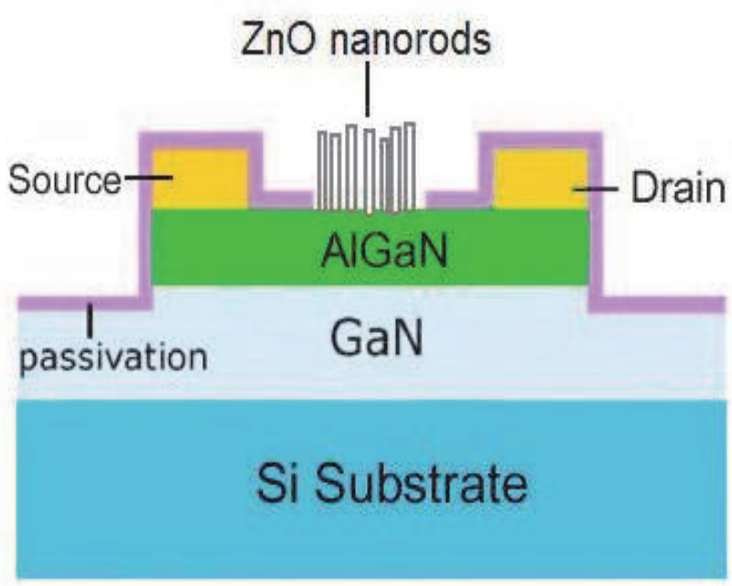

Fig. 24. Schematic cross sectional view of the ZnO nanorod gated HEMT for lactic acid detection.

The AlGaN/GaN HEMT drain-source current showed a rapid response when various concentrations of lactate acid solutions were introduced to the gate area of the HEMT sensor. The HEMT could detect lactate acid concentrations from 167 nM to 139 μM. Figure 25 shows a real time detection of lactate acid by measuring the HEMT drain current at a constant drain-source bias voltage of 500 mV during exposure of HEMT sensor to solutions with different concentrations of lactate acid. The sensor was first exposed to 20 l of 10 mM PBS and no current change could be detected with the addition of 10 l of PBS at approximately 40 seconds, showing the specificity and stability of the device. By contrast, a rapid increase in the drain current was observed when target lactate acid was introduced to the device surface. The sensor was continuously exposed to lactate acid concentrations from 167 nM to 139 μM.

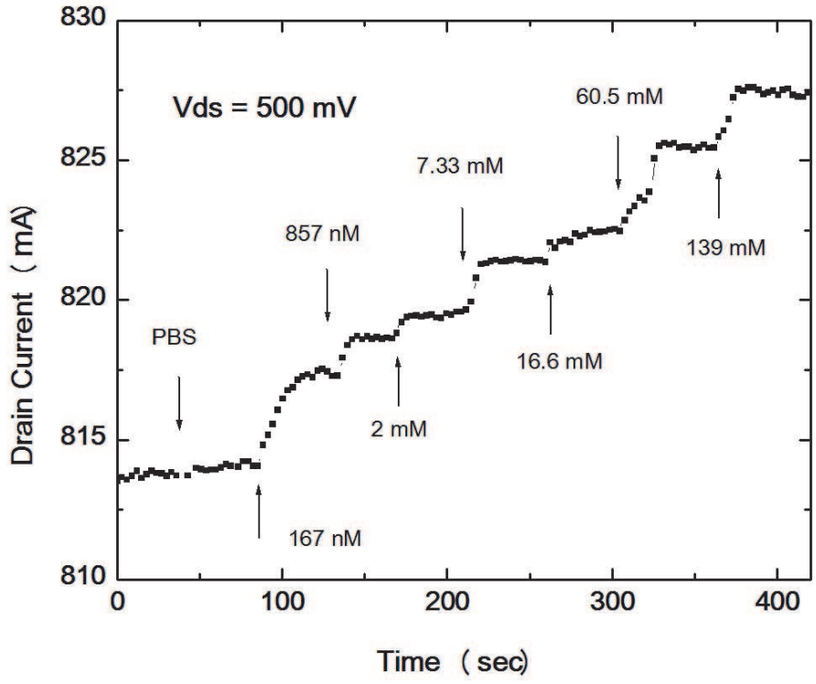

Fig. 25. Drain current as a function of the time with successive exposure to lactate acid from 167 nM to 139 M.

As compared with the amperometric measurement based lactate acid sensors, our HEMT sensors do not require a fixed reference electrode in the solution to measure the potential applied between the nano-materials and the reference electrode. The lactate acid sensing with the HEMT sensor was measured through the drain current of HEMT with a change of the charges on the ZnO nanorods and the detection signal was amplified through the HEMT. Although the time response of the HEMT sensors is similar to that of electrochemical based sensors, a significant change of drain current was observed for exposing the HEMT to the lactate acid at a low concentration of 167 nM due to this amplification effect. In addition, the amount of sample, which is dependent on the area of gate dimension, can be minimized for the HEMT sensor due to fact no reference electrode is required. Thus, measuring lactate acid in the exhaled breath condensate (EBC) can be achieved as a noninvasive method.

7.5 Chloride ion detection

Chlorine is widely used in the manufacture of many products and items directly or indirectly, i.e. in paper product production, antiseptic, dye-stuffs, food, insecticides, paints, petroleum products, plastics, medicines, textiles, solvents, and many other consumer products. It is used to kill bacteria and other microbes in drinking water supplies and waste water treatment. Excess chlorine also reacts with organics and forms disinfection by-products such as carcinogenic chloroform, which is harmful to human health. Thus, to ensure the safety of public health, it is very important to accurately and effectively monitor chlorine residues, typically in the form of chloride ion concentration, during the treatment and transport of drinking water (Taylor and Hong 2000, Walker, Hall and Hurst 1990, Cook and Miles 1980, Elsheimer 1987, Verma and Parthasarathy 1996, Graule et al. 1989, Kumar, Venkatesh and Maiti 2004, Blackwell et al. 1997). In addition, the chloride ion is an essential mineral for humans, and is maintained to a total body chloride balance in body fluids such as serum, blood, urine, exhaled breath condensate etc., by the kidneys. Variations in the chloride ion concentration in serum may serve as an index of renal diseases, adrenalism, pneumonia and, thus, the measurement of this parameter is clinically important (Walker et al. 1990, Davidsson et al. 2005, Davidsson et al. 2007, Niimi et al. 2004, Effros et al. 2002).

7.5.1 HEMT Functionalized with Ag/AgCl

(HEMTs) with a Ag/AgCl gate are found to exhibit significant changes in channel conductance upon exposing the gate region to various concentrations of chorine ion solutions, as shown in Figure 26. The Ag/AgCl gate electrode, prepared by potentiostatic anodization, changes electrical potential when it encounters chorine ions. This gate potential changes lead to a change of surface charge in the gate region of the HEMT, inducing a higher positive charge on the AlGaN surface, and increasing the pizeo-induced charge density in the HEMT channel. These anions create an image positive charge on the Ag gate metal for the required neutrality, thus increasing the drain current of the HEMT. The HEMT source-drain current showed a clear dependence on the chorine concentration (Walker et al. 1990).

Figure 27 shows the time dependence of Ag/AgCl HEMT drain current at a constant drain bias voltage of 500mV during exposure to solutions with different chlorine ion concentrations. The HEMT sensor was first exposed to DI water and no change of the drain current was detected with the addition of DI water at 100 seconds. This stability was important to exclude possible noise from the mechanical change of the NaCl solution. By sharp contrast, there was a rapid response of HEMT drain current observed in less than 30 seconds when target of 1×10^{-8} M NaCl solution was switched to the surface at 175 sec. The abrupt current change due to the exposure of chlorine in NaCl solution stabilized after the chlorine thoroughly diffused into the water to reach a steady state. When Ag/AgCl gate metal encountered chorine ions, the electrical potential of the gate was changed, inducing a higher positive charge on the AlGaN surface, and increased the pizeo-induced charge density in the HEMT channel. 1×10^{-7} M of NaCl solution was then applied at 382 second and it was accompanied with a larger signal corresponding to the higher chlorine concentration. Further real time tests were carried out to explore the detection of higher Cl^- ion concentrations. The sensors was exposed to 10^{-8} M, 10^{-7} M, 10^{-6} M, 10^{-5} M and 10^{-4} M solutions continuously and repeated five times to obtain the standard deviation of source-drain current response for each concentration. The limit of detection of this device was $1\times10^{-}$

^{8} M chlorine in DI-water. Between each test, the device was rinsed with DI water. These results suggest that our HEMT sensors are recyclable with simple DI water rinse. The presence of the Ag/AgCl gate leads to a logarithmic dependence of current on the concentration of NaCl.

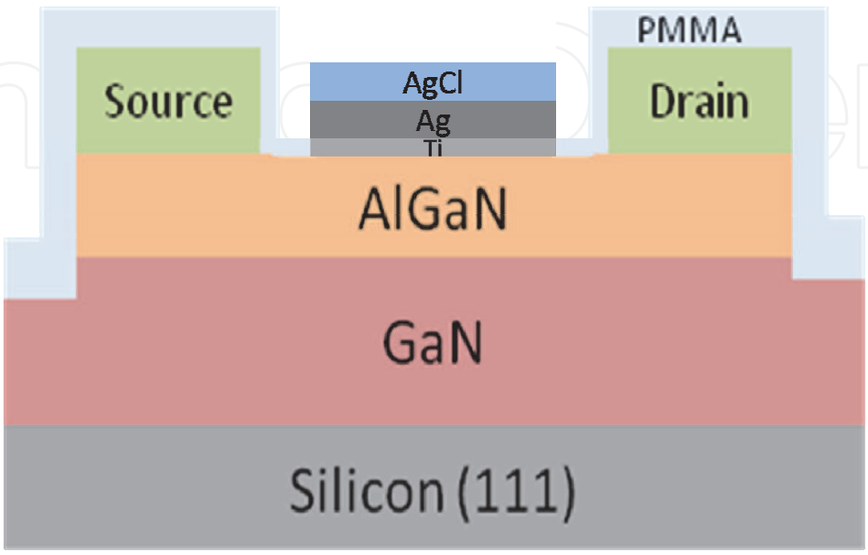

Fig. 26. Schematic cross sectional view of a Ag/AgCl gated HEMT.

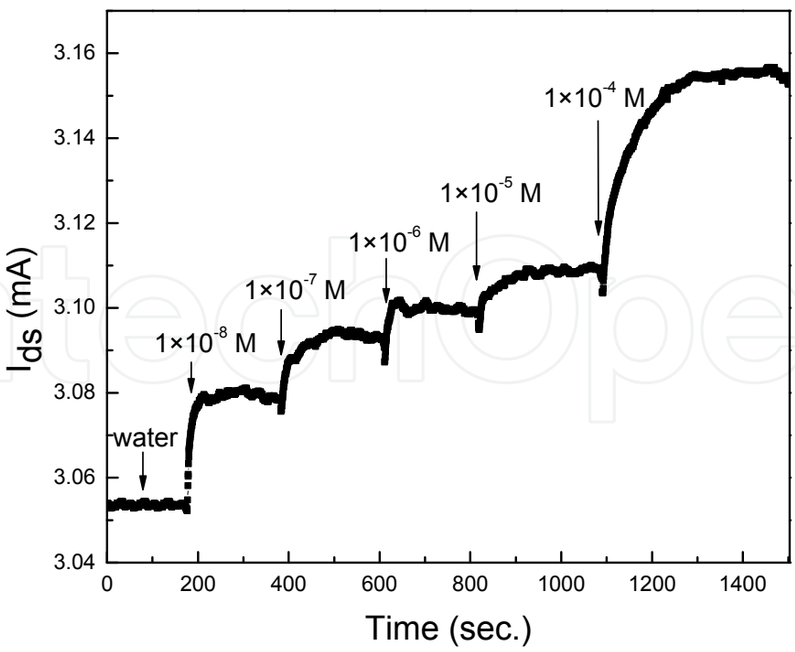

Fig. 27. Time dependent drain current of a Ag/AgCl gated AlGaN/GaN HEMT exposed to different concentrations of NaCl solutions (bottom).

7.5.2 HEMT Functionalized with InN

Real time detection of chloride ion detection with AlGaN/GaN high electron mobility transistors (HEMTs) with an InN thin film in the gate region has also been demonstrated. The sensor, shown schematically in Figure 28, exhibited significant changes in channel conductance upon exposure to various concentrations of NaCl solutions. The InN thin film, deposited by Molecular Beam Epitaxy, provided fixed surface sites for reversible anion coordination. The potential change in the gate area induced a change of the piezo-induced charge density in the electron channel in the HEMT. The sensor was tested over the range of 100nM to 100μM NaCl solutions.

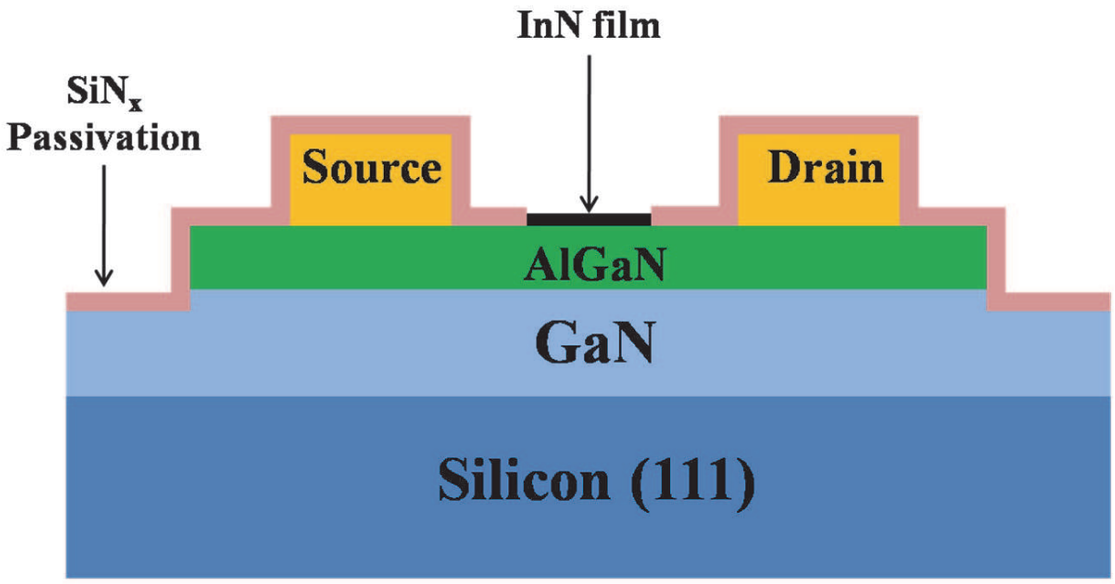

Fig. 28. Cross section schematic of the InN-gated HEMT.

Figure 29 also shows the results of real time detection of Cl^- ions by measuring the HEMT drain current at a constant drain bias voltage of 500mV during exposure to solutions of different chloride ion concentrations. The HEMT sensor was first exposed to DI water and no change of the drain current was detected with the addition of DI water at 100 seconds. The small spike in the current is due to mechanical disturbance of the HEMT surface when the water was added. By sharp contrast, a rapid response of HEMT drain current was observed in less than 20 seconds when target of 100 nM NaCl solution was exposed to the surface at 200 seconds. The abrupt current change stabilized after the sodium chloride solution thoroughly diffused into water and reached a steady state. When the InN gate metal encountered chloride ion, the electrical potential of the gate was changed and resulted in the increase the pizeo-induced charge density in the HEMT channel. A larger signal change was observed when 1μM of NaCl solution was applied at 300 seconds. The sensor was exposed to higher Cl^- ion concentrations of 10μM and 100μM sequentially for a further real time test. The test was repeated with the same sensor for five times to obtain the standard deviation of source-drain current response for each concentration. The sensor can be reusable by washing it with DI water and drying with nitrogen gas. The limit of detection of this device was 100nM chloride ions in DI water. The presence of the InN gate leads to a logarithmic dependence of current on the concentration for NaCl.

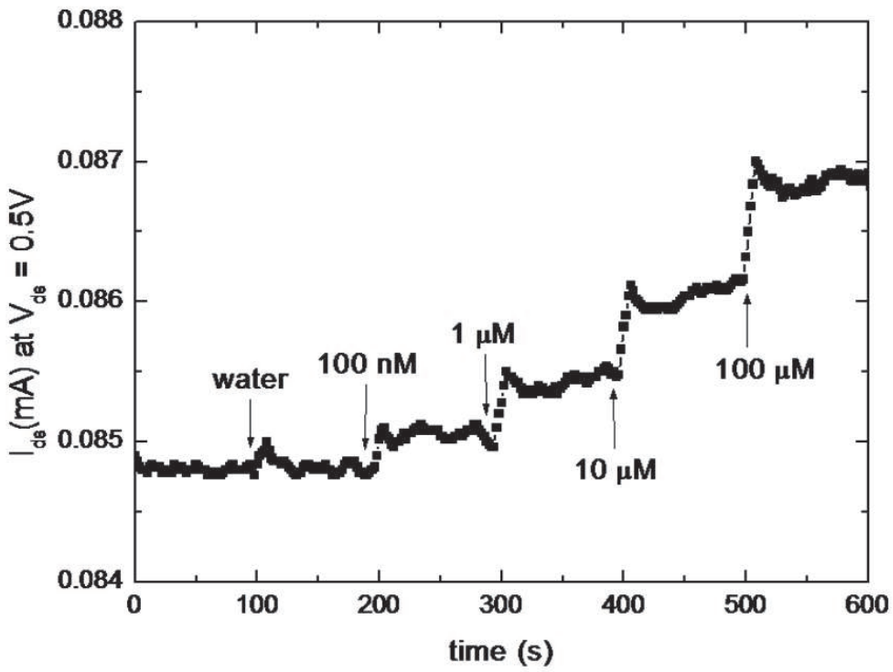

Fig. 29. Real time source-drain current at a constant bias of 500mV as different concentrations of Cl- ions were added.

7.6 Traumatic Brain Injury

TBI is one of the most frequent causes of morbidity and mortality on the modern battlefield. U.S. casualties in Iraq are suffering a greater percentage of brain injuries than in previous wars. One of the contributing factors is the proliferation of the use of Improvised Explosive Device (IED) against US warfighters (Warden , Langlois, Rutland-Brown and Thomas 2004). Recent assessments have indicated that about 65 % of casualties are correlated with brain injuries. Traumatic brain injury, including concussion are also growing medical problem among civilians, with almost 2 million cases in the US each year (Langlois et al. 2004). The development of a fast response and portable TBI sensor can have tremendous impact in early diagnosis, and proper management of TBI. Accurate and early diagnosis of a soldier's health in acute care environments can significantly simplify decisions about situation management. For example, decisions need to be made about whether to admit or discharge injured soldiers or to transfer other facility with advanced diagonal system, such as computer tomography (CT) and magnetic resonance imaging (MRI) scans. The capability to detect, in real time, markers in body fluids of soldiers can result in better patient outcomes especially in the battlefield or remote areas, where complicated and expensive CT and MRI scans are not available. For example, traumatic brain injury (TBI) is one of the most frequent causes of morbidity and mortality on the modern battlefield (Warden , Langlois et al. 2004). U.S. casualties in Iraq are suffering a greater percentage of brain injuries than in previous wars. Recent assessments have indicated that about 65 % of casualties are correlated with brain injuries, and concussion is a growing medical problem. The development of a fast response and portable TBI sensor can have tremendous impact in early diagnosis, and proper management of TBI

Preliminary results show the TBI antibody can be functionalized on the HEMT surface and fast response of TBI antigen was achieved. The detection of limit of detection (LOD) was in the 10th of g/ml range, however this is not low enough for practical use. The typical TBI antigen concentration in the TBI patient's serum is in the range of ng/ml. We have used HEMT sensors to detect the kidney injury molecules and prostate specific antigen and achieved the LOD in the range of 1-10 pg/ml range. The reason for higher LOD for the TBI antigen detection was due to the much smaller size of the TBI antigen. Smaller antigens carry less charges, thus provide less effect on the drain current of the HEMT sensor. Based on the promising biomarker and device data, we have recently used HEMTs for detecting a biomarker UCH-L1 (BA0127) antigen involved in Traumatic Injury Molecule. The gate region was functionalized with a specific antibody to traumatic brain injury antigen. The HEMT current showed a decrease as a function of TBI antigen concentration in PBS buffer (Figure 30). This shows the time dependent current change in BA0127 (UCH-L1) antibody modified HEMTs upon exposure to 2 μg/ml, and then to 16.9, 80, and 188 μg/ml of BA0127 (UCH-L1) in PBS buffer. The response time is around 6 seconds. The preliminary limit of detection (LOD) was found to be 20 μg/ml, demonstrating the potential for TBI detection with accurate, rapid, noninvasive, and high throughput capabilities.

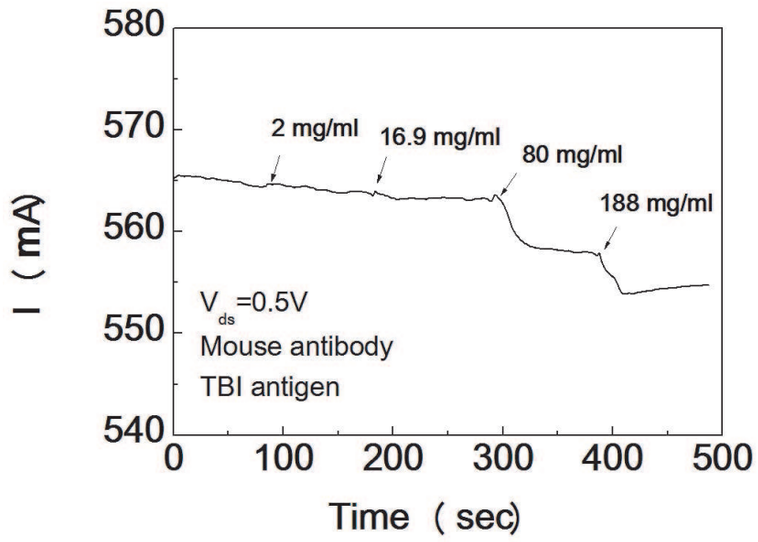

Fig. 30. Time dependent current signal when exposing the HEMT to 2 μg/ml to 188 μg/ml BA0127 TBI antigen in PBS buffer.

8. Endocrine disrupter exposure level meassurement

There have been many reports evaluating the adverse effects of endocrine disrupters (ED) on reproduction in wild animals, especially in aquatic environments (Mosconi et al. 2002, Sumpter and Jobling 1995, Matozzo et al. 2008a, Watson et al. 2007, Garcia-Reyero et al. 2006, Porte et al. 2006, Hinck et al. 2008). A wide range of chemicals are considered EDs, including naturally occurring or improperly disposed estrogens and anthropogenic chemicals that were heavily used in the past. These chemicals promote feminization in wild life and also pose a threat to public health. Some reports suggest that ED can influence fetal development (Bern 1998) or act as a carcinogen (Davis et al. 1993, Yager and Liehr 1996,

Liehlr 2001). Therefore, it is beneficial to develop tools that could accurately monitor the level of ED exposure.

Vitellogenin (Vtg) is a major egg yolk precursor protein that can be used as a biomarker to indicate an organism's exposure to ED (Heppell et al. 1995). The gene for this protein is expressed in the liver of oviparous animals under the control of estrogen (Matozzo et al. 2008b, Heppell et al. 1995, Carmon, Baltus and Luck 2005b, Hahn et al. 2006, Eidem et al. 2006, Sabo-Attwood et al. 2007, Denslow et al. 1999, Garcia-Reyero et al. 2009, Chertow et al. 1998). Male fish, under natural conditions, should have very low doses of Vtg since they do not produce eggs. However, if male fish are exposed to estrogen or to estrogen mimics in the environment, the Vtg gene is turned on. The dynamic range of this protein in normal male fish is 10-50 ng/ml in plasma and ~20 mg/ml in females producing eggs (Denslow et al. 1999). There have been reports of finding as much as 100 mg/ml in some fish that were induced with estrogen (Garcia-Reyero et al. 2009). While the dynamic range is over 6 orders of magnitude, one normally finds 1~100 g/ml in plasma in exposed males (Denslow et al. 1999). Although Vtg from one species is limited in its application as a probe for another, some segments of Vtg are highly conserved among species, suggesting the possibility of developing antibodies with wide cross-reactivity (Denslow et al. 1999). Enzyme-linked-immunosorbent-assay (ELISA) (Heppell et al. 1995, Eidem et al. 2006, Sabo-Attwood et al. 2007, Denslow et al. 1999, Garcia-Reyero et al. 2009), quartz crystal microbalance (Carmon, Baltus and Luck 2005a), and yeast cell-based assay (Hahn et al. 2006) are typically used as the Vtg detection methods, however, these methods are not suitable for on-field, real-time measurements.

Figure 31 shows the results of real time detection of Vtg by measuring the HEMT at constant drain bias voltage of 500 mV with an Agilent 4156C parameter analyzer at 25°C. Purified Vtg solutions were prepared in 10mM PBS and introduced to the sensor surface by a syringe autopipette (0.5-2μL). The drain current measurement began with 10 μL of PBS placing on the HEMT surface. Before introducing the Vtg solutions, an additional 1μL drop of PBS was added to the sensor. Other than the small disturbance at 50 seconds, no change of the drain current was detected. The disturbance in the current was due to mechanical disturbance of the HEMT surface and the level went back to its original state. In comparison, a rapid response of HEMT drain current was observed in less than 10 seconds when the sensor was exposed to 5μg/mL of Vtg at 100 seconds. The abrupt current change stabilized after the VTG thoroughly diffused into the solution and reached a steady state. When the antigen encountered the antibody, the electrical potential of the gate was changed and resulted in the increase of the pizeo-induced charge density in the HEMT channel.

A larger signal change was observed when 10μg/mL of Vtg was added at 200 seconds. There was PBS solution on the sensor already. In order to achieve the 10μg/mL of Vtg on the sensor, higher concentration than 10μg/mL was needed to be used to add on the sensor. Thus, an abrupt spike of the drain current change was observed due to the exposure of higher Vtg concentration solution to the sensing area, which was stabilized after the Vtg thoroughly diffused into the solution on the top of the sensing area. The sensor was exposed to higher Vtg concentrations of 50μg/mL and 100μg/mL sequentially for further real time test. The test was repeated with the same sensor for three times. The sensors were rinsed with 10mM PBS at pH=6 because antibodies have optimal reactivity at pH=7.4 and will release the antigen at a lower pH.

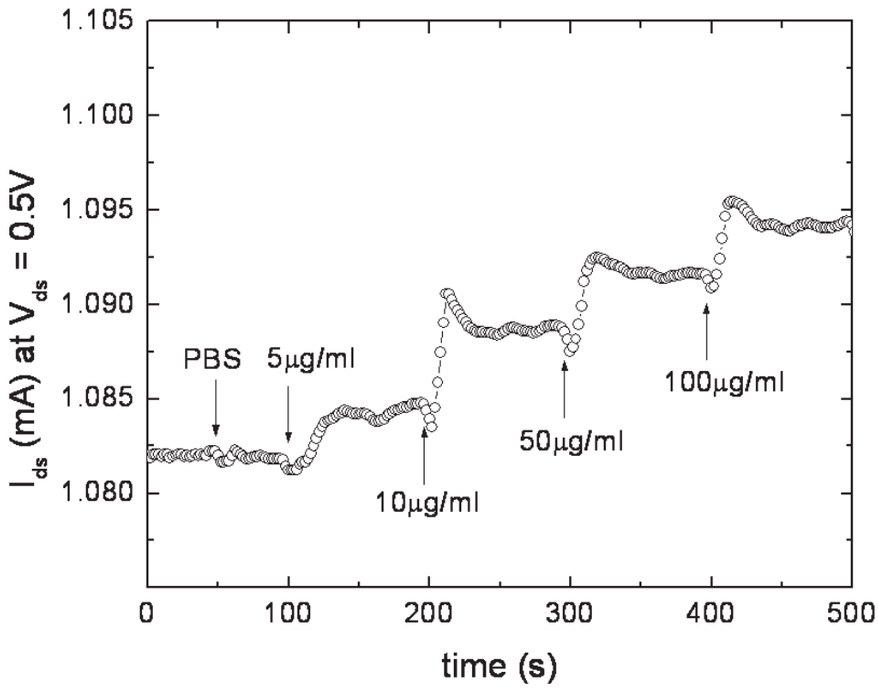

Fig. 31. Real time source-drain current of sensors when introduced to 5, 10, 50, and 100 μg/mL of vitellogenin

Figure 32 (top) shows Vtg detection results with actual male and female largemouth bass serum samples. The male serum contained no vitellogenin whereas the female serum contained 8mg/mL of Vtg. In contrast to PBS solutions, serum has many proteins that can interfere with the correct sensor reading. Therefore, it was necessary to block the unreacted carboxylic groups on the sensor. 1mg/mL bovine serum albumin (BSA) solution was applied to the sensor for 3 hours and washed thoroughly with PBS to remove the excess BSA. An important factor that influences the sensor performance is the Debye length of the solution (Curreli et al. 2008). Electrolytes that are present in the solution can screen the field effect from the antigen-antibody interaction. In solutions such as serum, the Debye length is greatly reduced and causes lower sensitivity of the device. Therefore, dilution of largemouth bass serum was needed to detect Vtg in the solution. The serum was diluted to 1% in 10mM PBS. The measurement started with 1% male serum containing no Vtg on the sensor. At 100 seconds, additional diluted male serum was added to confirm that there was no current change due to the serum background. By contrast, the current increased when drops of 1% female serum containing Vtg were added every 100 seconds.

Figure 32 (bottom) shows the drain current changes as a function of the Vtg concentration. Each concentration was repeated five times to obtain the standard deviation of source-drain current response for each concentration. The source-drain current change is nonlinearly proportional to Vtg concentration. Between each test, the device was rinsed with a wash buffer of 10 M phosphate buffer solution containing 10 M KCl with pH 6 to strip the antigen from the antibody. Successful detection in serum samples shows that HEMTs have potential as biological sensors in real-world applications.

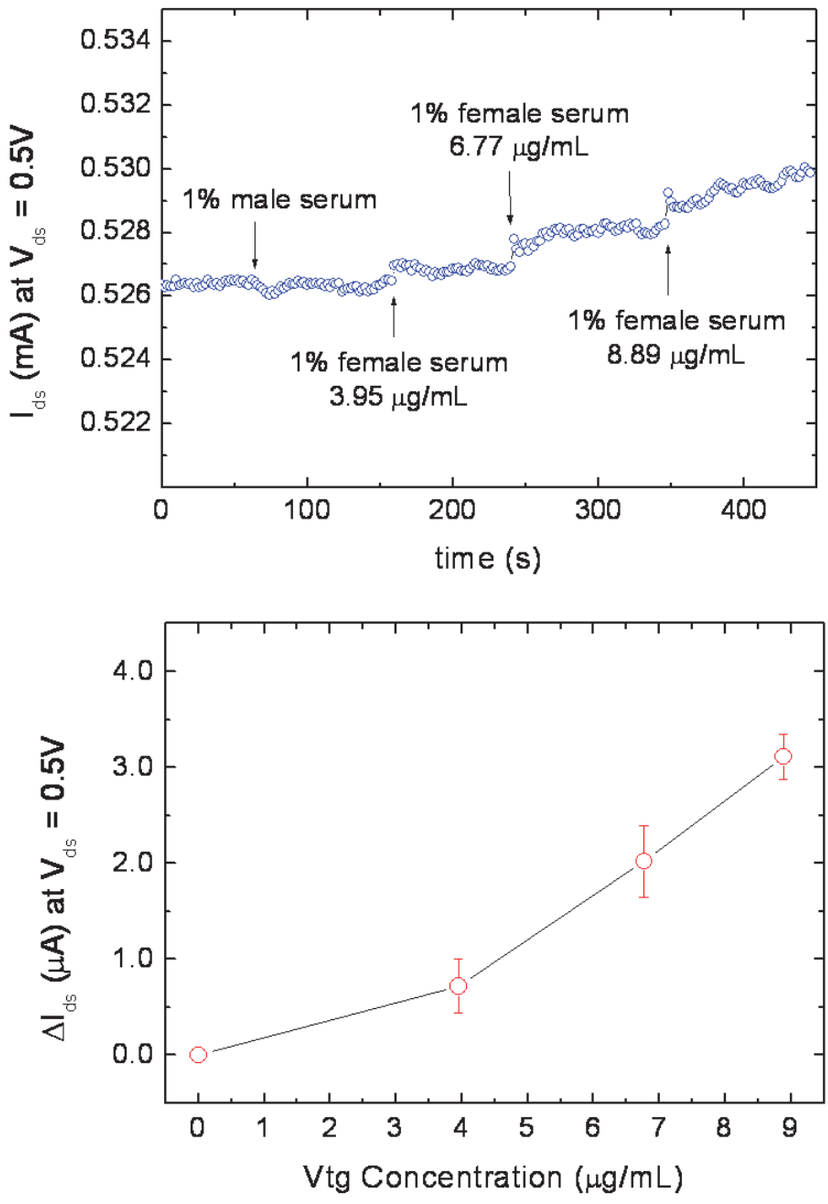

Fig. 32. (top) Real time detection of vitellogenin in largemouth bass serum. (bottom) Drain current change in HEMT as a function of vitellogenin concentration

9. Wireless sensors

With many of the sensor applications, it is desirable to have the detected signal transmitted wirelessly to a central location. This could be part of an unmanned system for biotoxin detection or part of a personal medical monitoring system in which a patient could breathe into a hand-held device that then transmits the encrypted signal to a doctor's office. This would allow for less numerous visits to doctor's offices and less problems with false positive

tests because data could be accumulated over an extended period and a more reliable baseline established.

A prototype of a remote hydrogen sensing system was installed in a Ford dealership in Orlando (Greenway Ford), which is a test site for a hydrogen-fueled vehicle program supported by Florida State Government, since August 2006. The hydrogen-fueled buses and cars are stored and have maintenance performed on them in a large work area at the Ford dealership. Our hydrogen sensing system includes four on-site sensors, power management subsystem, wireless transmitter and receiver connect to a computer. An intelligent monitoring software developed by our team is used to control data logging and tracking of each individual sensor as well as defining and implementing the monitoring states, transitions, and actions of the hydrogen sensor network. It can trigger an alarm and/or send messages to computers, cell phones or PDAs, when a preset hydrogen threshold level is detected. Also, the software is able to warn the users of potential sensor failure, power outages and network failures through cell phone network and Internet. Currently, the cost of electronic parts including wireless transceiver and detection circuits is less than $20 in small quantity. In large quantity, it can be lower than $10. If the complete wireless transceiver and detection circuit are designed and integrated on a custom IC for mass production, the cost should be in the range of $5-8, similar to Bluetooth wireless chips. The sensors themselves can be mass-produced for 5-10 cents each according to Nitronex, Inc. A schematic block diagram of sensor module and wireless network server is shown in Figure 33.

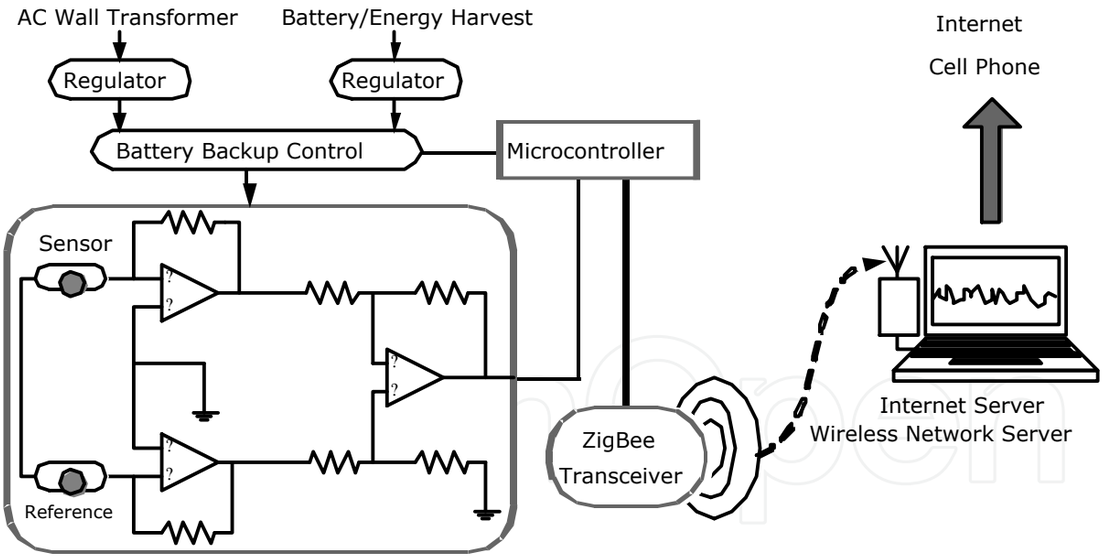

Fig. 33. Schematic of remote data transmission system for sensors.

As shown in the Figure 34, we have also developed a pen-sized portable, re-configurable wireless transceiver integrated with pH sensor has been designed and fabricated. The wireless transmitter and receiver pair was designed to acquire EBC data and transmit it wirelessly. This system is able to interface multiple different sensors and consists of a transmitter and receiver pair. The transmitter was designed such that it is the size of a marker-pen so that it could be used as an ultra-portable lightweight handheld device. The

transmitter is designed to be operated on an ultra-low-power mode. The transmitter is also equipped with an on-board recharging circuit, which can be powered by using a standard mini-USB cable. The transmitter consumes on average 80μA. The transmitter and receiver pair is designed to operate at 2.4GHz with range of up to 20ft line-of-sight. The receiver has USB 2.0 connectivity, which relays EBC data from the transmitter to a PC while powering the receiver. The transmitter is designed to integrate with various different sensors through a connector. The transmitter can be reset for the required input signal range to trigger the alarm through the bi-directional wireless communication for a different sensing application. Thus this system is reconfigurable over-the-air. The wireless circuits only consume a power level around 1 W. If the sensor consumes a similar power level, the battery installed on the transmitter package can last more than one month. This EBC sensing pair of devices can be mass-produced cost effectively well below $100 each pair. The sensor occupies the tip of the pen-shaped layout in Figure 34 and runs off a 75mA Li ion polymer rechargeable battery. Figure 34 illustrated the package sensors mounted on a circuit board containing the detection circuit and microcontroller and the wireless transmitter for data collection. The sensor module is fully integrated on an FR4 PC board and is packaged with battery. The dimension of the sensor module package is: 4.5" × 2.9" × 2". The maximum line of sight range between the sensor module and the base station is 150m. The base station of the wireless sensor network server is also integrated in a single module (3.0" × 2.7" × 1.1") and is ready to be connected to a laptop by a USB cable. The base station draws its power from the laptop's USB interface, thus do not require any battery or wall AC transformer, which reduces its form factor. The PC is used to record the sensing data, send the data to internet, and take actions when the hydrogen is detected.

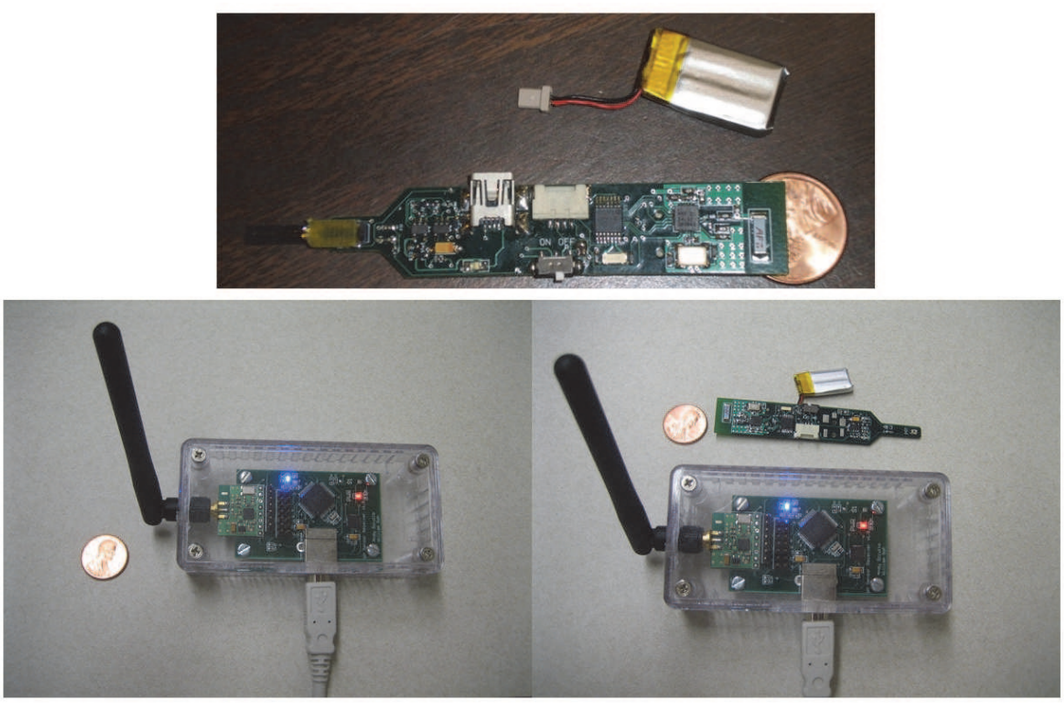

Fig. 34. Photographs of integrated pH sensor (top) and receiver/transmitter pair (bottom).

A client program has also been developed to receive the sensor data remotely. The remote client can get a real-time log of the system for 10 minutes via the client program. In addition, a full data log will be obtained via accessing the server using a ftp client as the server program incorporates a full data logging functionality. When the current of any of the sensors exceeds a preset level, the server program will automatically execute the phone-dialing program, reporting the emergency to relevant personnel. A web server was developed using MATLAB (Mathworks Inc) to share the collected sensor data via the Internet. The data display time range can be chosen real-time, 85 minutes, 15 hours and 6 day.

10. Summary

We have summarized recent progress in AlGaN/GaN HEMT sensors. These devices can take advantage of the advantages of microelectronics, including high sensitivity, possibility of high-density integration, and mass manufacturability. The goal is to realize real-time, portable and inexpensive chemical and biological sensors and to use these as handheld exhaled breath, saliva, urine, or blood monitors with wireless capability. Frequent screening can catch the early development of diseases, reduce the suffering of the patients due to late diagnoses, and lower the medical cost. For example, a 96 % survival rate has been predicted in breast cancer patients if the frequency of screening is every three months. This frequency cannot be achieved with current methods of mammography due to high cost to the patient and invasiveness (radiation).

There are many possible applications, including:

Diabetes/Glucose Testing -The population of diabetics is large and growing. There are in excess of 150 million diabetics in the world and some believe this number will double by 2010. Although the frequent monitoring of glucose levels is strongly encouraged by health professionals most of the glucose testing products currently on the market are uncomfortable for the user and dissatisfaction is high. Less invasive products are also less effective and have been unable to gain market share. Conditions are favorable for the introduction of an effective, non-invasive product.

Breast Cancer Testing - The market size for breast cancer testing is vast – nearly 200,000 women and 1,700 men were diagnosed in 2006 alone. Although lucrative, competition in this industry is strong. Growth potential is possible, however, as the most effective and widely used diagnostic exam for breast cancer, the mammogram, is potentially harmful due to radiation exposure. Other, less popular, exams that do not involve radiation tend to be both invasive and expensive.

Asthma Testing - Asthma testing products are increasingly in demand. 1 in 20 Americans suffers from asthma and this number stands to increase in the near future. Despite this, the market for pre-attack testing materials is undersaturated. Only one product has reached the marketplace and although inexpensive this product is also relatively inaccurate. Other potential competition may be more accurate but has yet to reach the market.

Prostate Testing - Because 1 in 6 men will be diagnosed with prostate cancer during his lifetime, the market for testing products is also quite large. While two tests currently possess the bulk of the market, they either inaccurate or invasive or both. Because of this relatively weak competitive market new entry possibilities are strong.

Narcotics Testing - Toxicology screens are the most common narcotics testing products currently on the market. Used regularly by law enforcement agencies, medical facilities, and

corporate businesses tests are inexpensive and effective. More advanced technology has also been developed to in an effort to monitor discrete drug levels in an individual's system.
HEMT sensors show promising results for protein, DNA, prostate cancer, kidney injury molecules, pH values of solutions, mercury ions as well glucose in the exhaled breath condensate. The method relies on an amplification of small changes in antibody-structure due to binding to antigens. The characteristics of these sensors include fast response (liquid phase-5 to 10 seconds and gas phase- milli-second), digital output signal, small device size (less than 100 100 m^2) and chemical and thermal stability.
Given the ever increasing incidence of diabetes in both the United States and abroad the market for diabetes testing and supplies is large and growing. Moreover, prevalent market-wide dissatisfaction with current testing alternatives – due to discomfort, inaccuracy, and/or cost – leads us to believe that the diabetes testing market is by far the most promising one for this technology. Although possible concerns include a difficult government certification process and insurance coverage, a survey of possible competition shows similar products to be either nonexistent or in an embryonic stage of development, meaning possible market entry can be made carefully and strategically.
Like the market for diabetes testing, the market for breast cancer testing is also highly promising. Although numerous testing alternatives exist the market size is huge and growing – in 2005 the testing market in the United States alone was worth well in excess of $1 billion – and the most common diagnostic methods involve some level of discomfort and/or exposure to radiation giving it the same kind of patient dissatisfaction found among diabetes. Because testing is performed less frequently, however, its larger market may prove less lucrative and market entry is highly dependent upon government regulations and insurance coverage. Barring these difficulties market entry (if made carefully) should be relatively easy.
There are still some critical issues. First, the sensitivity for certain antigens (such as prostate or breast cancer) needs to be improved further to allow sensing in body fluids other than blood (urine, saliva). Second, a sandwich assay allowing the detection of the same antigen using two different antibodies (similar to ELISA) needs to be tested. Third, integrating multiple sensors on a single chip with automated fluid handling and algorithms to analyze multiple detection signals, and fourth, a package that will result in a cheap final product is needed. Fourth, the stability of surface functionalization layers in some cases is not conducive to long-term storage and this will limit the applicability of those sensors outside of clinics. There is certainly a need for detection of multiple analytes simultaneously. However, there are many such approaches and acceptance from the clinical community is generally slow for many reasons, including regulatory concerns.

11. Acknowledgments

The work at UF is partially supported by the Office of Naval Research (ONR) under Contract number 00075094 monitored by Dr. Chagaan Baatar, NSF under contract number ECCS 0901711 monitored by Dr. Yogesh B. Gianchandani, NASA Kennedy Space Center Grant NAG 10-316 monitored by Mr. Daniel E. Fitch, and by Superfund Basic Research Program Grant RO1ES015449.

12. References

Learn About Cancer. American Cancer Society.
What is Breast Cancer? United States Department of Health and Human Services.

Accordino, R., A. Visentin, A. Bordin, S. Ferrazzoni, E. Marian, F. Rizzato, C. Canova, R. Venturini & P. Maestrelli (2008) Long-term repeatability of exhaled breath condensate pH in asthma. *Respiratory Medicine,* 102**,** 377-381.

Anderson, J. L., E. F. Bowden & P. G. Pickup (1996) Dynamic electrochemistry: Methodology and application. *Analytical Chemistry,* 68**,** R379-R444.

Anderson, T., F. Ren, S. Pearton, B. Kang, H. Wang, C. Chang & J. Lin (2009) Advances in Hydrogen, Carbon Dioxide, and Hydrocarbon Gas Sensor Technology Using GaN and ZnO-Based Devices. *Sensors,* 9**,** 4669-4694.

Anderson, T., H. Wang, B. Kang, F. Ren, S. Pearton, A. Osinsky, A. Dabiran & P. Chow (2008) Effect of bias voltage polarity on hydrogen sensing with AlGaN/GaN Schottky diodes. *APPLIED SURFACE SCIENCE,* 255**,** 2524-2526.

Anh, D. T. V., W. Olthuis & P. Bergveld (2005) A hydrogen peroxide sensor for exhaled breath measurement. *Sensors and Actuators B-Chemical,* 111**,** 494-499.

Arnon, S. S., R. Schechter, T. V. Inglesby, D. A. Henderson, J. G. Bartlett, M. S. Ascher, E. Eitzen, A. D. Fine, J. Hauer, M. Layton, S. Lillibridge, M. T. Osterholm, T. O'Toole, G. Parker, T. M. Perl, P. K. Russell, D. L. Swerdlow, K. Tonat & B. Working Grp Civilian (2001) Botulinum toxin as a biological weapon - Medical and public health management. *Jama-Journal of the American Medical Association,* 285**,** 1059-1070.

Bagramyan, K., J. R. Barash, S. S. Arnon & M. Kalkum (2008) Attomolar Detection of Botulinum Toxin Type A in Complex Biological Matrices. *Plos One,* 3.

Bermudez, J. 2001. *The armed forces of North Korea*. IB Tauris.

Bern, H. A. (1998) The fragile fetus. *Journal of Clean Technology Environmental Toxicology and Occupational Medicine,* 7**,** 25-32.

Bigler, L. R., C. F. Streckfus, L. Copeland, R. Burns, X. L. Dai, M. Kuhn, P. Martin & S. A. Bigler (2002) The potential use of saliva to detect recurrence of disease in women with breast carcinoma. *Journal of Oral Pathology & Medicine,* 31**,** 421-431.

Blackwell, P. A., M. R. Cave, A. E. Davis & S. A. Malik (1997) Determination of chlorine and bromine in rocks by alkaline fusion with ion chromatography detection. *Journal of Chromatography A,* 770**,** 93-98.

Bloemen, K., G. Lissens, K. Desager & G. Schoeters (2007) Determinants of variability of protein content, volume and pH of exhaled breath condensate. *Respiratory Medicine,* 101**,** 1331-1337.

Bonventre, J. V. & J. M. Weinberg (2003) Recent advances in the pathophysiology of ischemic acute renal failure. *Journal of the American Society of Nephrology,* 14**,** 2199-2210.

Burlingame, A., R. Boyd & S. Gaskell (1996) Mass Spectrometry. *Anal. Chem,* 68**,** 599-652.

Carmon, K., R. Baltus & L. Luck (2005a) A biosensor for estrogenic substances using the quartz crystal microbalance. *ANALYTICAL BIOCHEMISTRY,* 345**,** 277-283.

Carmon, K. S., R. E. Baltus & L. A. Luck (2005b) A biosensor for estrogenic substances using the quartz crystal microbalance. *Analytical Biochemistry,* 345**,** 277-283.

Carpagnano, G. E., M. P. F. Barbaro, O. Resta, E. Gramiccioni, N. V. Valerio, P. Bracciale & G. Valerio (2005) Exhaled markers in the monitoring of airways inflammation and its response to steroid's treatment in mild persistent asthma. *European Journal of Pharmacology,* 519**,** 175-181.

Chase, W. R. (2000) Salivary markers: their role in breast cancer detection. *J Mich Dent Assoc,* 82**,** 12.

Chen, K., H. Wang, B. Kang, C. Chang, Y. Wang, T. Lele, F. Ren, S. Pearton, A. Dabiran, A. Osinsky & P. Chow (2008) Low Hg(II) ion concentration electrical detection with AlGaN/GaN high electron mobility transistors. *SENSORS AND ACTUATORS B-CHEMICAL,* 134**,** 386-389.

Chen, R. J., S. Bangsaruntip, K. A. Drouvalakis, N. W. S. Kam, M. Shim, Y. M. Li, W. Kim, P. J. Utz & H. J. Dai (2003) Noncovalent functionalization of carbon nanotubes for highly specific electronic biosensors. *Proceedings of the National Academy of Sciences of the United States of America,* 100**,** 4984-4989.

Chertow, G. M., E. M. Levy, K. E. Hammermeister, F. Grover & J. Daley (1998) Independent association between acute renal failure and mortality following cardiac surgery. *American Journal of Medicine,* 104**,** 343-348.

Cook, J. M. & D. L. Miles. 1980. Methods for the chemical analysis of groundwater, *Report, 80/5*. Institute of Geological. Sciences.

Cordesman, A. (1998) Weapons of mass destruction in the Gulf and greater Middle East: force trends, strategy, tactics and damage effects. *Washington DC: Center for Strategic and International Studies***,** 18–52.

Curreli, M., R. Zhang, F. N. Ishikawa, H. K. Chang, R. J. Cote, C. Zhou & M. E. Thompson (2008) Real-Time, Label-Free Detection of Biological Entities Using Nanowire-Based FETs. *Ieee Transactions on Nanotechnology,* 7**,** 651-667.

Czebe, K., I. Barta, B. Antus, M. Valyon, I. Horvath & T. Kullmann (2008) Influence of condensing equipment and temperature on exhaled breath condensate pH, total protein and leukotriene concentrations. *Respiratory Medicine,* 102**,** 720-725.

Davidsson, A., K. N. Sjosward, L. Lundman & B. Schmekel (2005) Quantitative assessment and repeatability of chlorine in exhaled breath condensate - Comparison of two types of condensators. *Respiration,* 72**,** 529-536.

Davidsson, A., M. Soderstrom, K. N. Sjosward & B. Schmekel (2007) Chlorine in breath condensate - A measure of airway affection in pollinosis? *Respiration,* 74**,** 184-191.

Davis, D. L., H. L. Bradlow, M. Wolff, T. Woodruff, D. G. Hoel & H. Antonculver (1993) MEDICAL HYPOTHESIS - XENOESTROGENS AS PREVENTABLE CAUSES OF BREAST-CANCER. *Environmental Health Perspectives,* 101**,** 372-377.

Denslow, N. D., M. C. Chow, K. J. Kroll & L. Green (1999) Vitellogenin as a biomarker of exposure for estrogen or estrogen mimics. *Ecotoxicology,* 8**,** 385-398.

Di, J. W., J. J. Cheng, Q. A. Xu, H. I. Zheng, J. Y. Zhuang, Y. B. Sun, K. Y. Wang, X. Y. Mo & S. P. Bi (2007) Direct electrochemistry of lactate dehydrogenase immobilized on silica sol-gel modified gold electrode and its application. *Biosensors & Bioelectronics,* 23**,** 682-687.

Effros, R. M., K. W. Hoagland, M. Bosbous, D. Castillo, B. Foss, M. Dunning, M. Gare, W. Lin & F. Sun (2002) Dilution of respiratory solutes in exhaled condensates. *American Journal of Respiratory and Critical Care Medicine,* 165**,** 663-669.

Eickhoff, M., J. Schalwig, G. Steinhoff, O. Weidemann, L. Görgens, R. Neuberger, M. Hermann, B. Baur, G. Müller & O. Ambacher (2003) Electronics and sensors based on pyroelectric AlGaN/GaN heterostructures–Part B: Sensor applications. *physica status solidi (c)***,** 1908-1918.

Eidem, J. K., H. Kleivdal, K. Kroll, N. Denslow, R. van Aerle, C. Tyler, G. Panter, T. Hutchinson & A. Goksoyr (2006) Development and validation of a direct

homologous quantitative sandwich ELISA for fathead minnow (Pimephales promelas) vitellogenin. *Aquatic Toxicology,* 78**,** 202-206.

Elsheimer, H. N. (1987) APPLICATION OF AN ION-SELECTIVE ELECTRODE METHOD TO THE DETERMINATION OF CHLORIDE IN 41 INTERNATIONAL GEOCHEMICAL REFERENCE MATERIALS. *Geostandards Newsletter,* 11**,** 115-122.

Fernández-Sánchez, C., C. McNeil, K. Rawson & O. Nilsson (2004) Disposable noncompetitive immunosensor for free and total prostate-specific antigen based on capacitance measurement. *Anal. Chem,* 76**,** 5649-5656.

Gangwani, P., S. Pandey, S. HaIdar, M. Gupta & R. S. Gupta (2007) Polarization dependent analysis of AlGaN/GaN HEMT for high power applications. *Solid-State Electronics,* 51**,** 130-135.

Garcia-Reyero, N., D. S. Barber, T. S. Gross, K. G. Johnson, M. S. Sepulveda, N. J. Szabo & N. D. Denslow (2006) Dietary exposure of largemouth bass to OCPs changes expression of genes important for reproduction. *Aquatic Toxicology,* 78**,** 358-369.

Garcia-Reyero, N., K. J. Kroll, L. Liu, E. F. Orlando, K. H. Watanabe, M. S. Sepulveda, D. L. Villeneuve, E. J. Perkins, G. T. Ankley & N. D. Denslow (2009) Gene expression responses in male fathead minnows exposed to binary mixtures of an estrogen and antiestrogen. *Bmc Genomics,* 10.

Gessner, C., S. Hammerschmidt, H. Kuhn, H. A. Seyfarth, U. Sack, L. Engelmann, J. Schauer & H. Wirtz (2003) Exhaled breath condensate acidification in acute lung injury. *Respiratory Medicine,* 97**,** 1188-1194.

Graule, T., A. Vonbohlen, J. A. C. Broekaert, E. Grallath, R. Klockenkamper, P. Tschopel & G. Tolg (1989) ATOMIC EMISSION AND ATOMIC-ABSORPTION SPECTROMETRIC ANALYSIS OF HIGH-PURITY POWDERS FOR THE PRODUCTION OF CERAMICS. *Fresenius Zeitschrift Fur Analytische Chemie,* 335**,** 637-642.

Greenfield, R. A., B. R. Brown, J. B. Hutchins, J. J. Iandolo, R. Jackson, L. N. Slater & M. S. Bronze (2002) Microbiological, biological, and chemical weapons of warfare and terrorism. *American Journal of the Medical Sciences,* 323**,** 326-340.

Haccoun, J., B. Piro, V. Noel & M. C. Pham (2006) The development of reagentless lactate biosensor based on a novel conducting polymer. *Bioelectrochemistry,* 68**,** 218-226.

Hahn, T., K. Tag, K. Riedel, S. Uhlig, K. Baronian, G. Gellissen & G. Kunze (2006) A novel estrogen sensor based on recombinant Arxula adeninivorans cells. *Biosensors & Bioelectronics,* 21**,** 2078-2085.

Han, D. I., D. S. Kim, J. E. Park, J. K. Shin, S. H. Kong, P. Choi, J. H. Lee & G. Lim (2005) Detection of streptavidin-biotin protein complexes using three-dimensional MOSFET in the Si micro-fluidic channel. *Japanese Journal of Applied Physics Part 1-Regular Papers Brief Communications & Review Papers,* 44**,** 5496-5499.

Harrison, T., L. Bigler, M. Tucci, L. Pratt, F. Malamud, J. T. Thigpen, C. Streckfus & H. Younger (1998) Salivary sIgA concentrations and stimulated whole saliva flow rates among women undergoing chemotherapy for breast cancer: an exploratory study. *Spec Care Dentist,* 18**,** 109-12.

Healy, D. A., C. J. Hayes, P. Leonard, L. McKenna & R. O'Kennedy (2007) Biosensor developments: application to prostate-specific antigen detection. *Trends in Biotechnology,* 25**,** 125-131.

Heppell, S. A., N. D. Denslow, L. C. Folmar & C. V. Sullivan (1995) UNIVERSAL ASSAY OF VITELLOGENIN AS A BIOMARKER FOR ENVIRONMENTAL ESTROGENS. *Environmental Health Perspectives,* 103**,** 9-15.

Hinck, J. E., V. S. Blazer, N. D. Denslow, K. R. Echols, R. W. Gale, C. Wieser, T. W. Maya, M. Ellersiecke, J. J. Coyle & D. E. Tillitt (2008) Chemical contaminants, health indicators, and reproductive biomarker responses in fish from rivers in the Southeastern United States. *Science of the Total Environment,* 390**,** 538-557.

Horvath, I., J. Hunt, P. J. Barnes & A. E. T. F. E. Breath (2005) Exhaled breath condensate: methodological recommendations and unresolved questions. *European Respiratory Journal,* 26**,** 523-548.

Hrapovic, S., Y. L. Liu, K. B. Male & J. H. T. Luong (2004) Electrochemical biosensing platforms using platinum nanoparticles and carbon nanotubes. *Analytical Chemistry,* 76**,** 1083-1088.

Huber, F., H. P. Lang & C. Gerber (2008) BIOSENSORS New leverage against superbugs. *Nature Nanotechnology,* 3**,** 645-646.

Hunt, J. F., K. Z. Fang, R. Malik, A. Snyder, N. Malhotra, T. A. E. Platts-Mills & B. Gaston (2000) Endogenous airway acidification - Implications for asthma pathophysiology. *American Journal of Respiratory and Critical Care Medicine,* 161**,** 694-699.

Hwang, K. S., J. H. Lee, J. Park, D. S. Yoon, J. H. Park & T. S. Kim (2004) In-situ quantitative analysis of a prostate-specific antigen (PSA) using a nanomechanical PZT cantilever. *Lab on a Chip,* 4**,** 547-552.

Ichimura, T., J. V. Bonventre, V. Bailly, H. Wei, C. A. Hession, R. L. Cate & M. Sanicola (1998) Kidney injury molecule-1 (KIM-1), a putative epithelial cell adhesion molecule containing a novel immunoglobulin domain, is up-regulated in renal cells after injury. *Journal of Biological Chemistry,* 273**,** 4135-4142.

Jackson, K. W. & G. R. Chen (1996) Atomic absorption, atomic emission, and flame emission spectrometry. *Analytical Chemistry,* 68**,** R231-R256.

Johnson, J., Y. H. Choi, A. Ural, W. Lim, J. S. Wright, B. P. Gila, F. Ren & S. J. Pearton (2009) Growth and Characterization of GaN Nanowires for Hydrogen Sensors. *Journal of Electronic Materials,* 38**,** 490-494.

Johnson, J. W., B. Luo, F. Ren, B. P. Gila, W. Krishnamoorthy, C. R. Abernathy, S. J. Pearton, J. I. Chyi, T. E. Nee, C. M. Lee & C. C. Chuo (2000) Gd2O3/GaN metal-oxide-semiconductor field-effect transistor. *Applied Physics Letters,* 77**,** 3230-3232.

Jun, J., B. Chou, J. Lin, A. Phipps, X. Shengwen, K. Ngo, D. Johnson, A. Kasyap, T. Nishida, H. T. Wang, B. S. Kang, F. Ren, L. C. Tien, P. W. Sadik, D. P. Norton, L. F. Voss & S. J. Pearton (2007) A hydrogen leakage detection system using self-powered wireless hydrogen sensor nodes. *Solid-State Electronics,* 51**,** 1018-1022.

Kang, B., S. Kim, F. Ren, J. Johnson, R. Therrien, P. Rajagopal, J. Roberts, E. Piner, K. Linthicum, S. Chu, K. Baik, B. Gila, C. Abernathy & S. Pearton (2004a) Pressure-induced changes in the conductivity of AlGaN/GaN high-electron mobility-transistor membranes. *APPLIED PHYSICS LETTERS,* 85**,** 2962-2964.

Kang, B., G. Louche, R. Duran, Y. Gnanou, S. Pearton & F. Ren (2004b) Gateless AlGaN/GaN HEMT response to block co-polymers. *SOLID-STATE ELECTRONICS,* 48**,** 851-854.

Kang, B., R. Mehandru, S. Kim, F. Ren, R. Fitch, J. Gillespie, N. Moser, G. Jessen, T. Jenkins & R. Dettmer (2005a) Hydrogen sensors based on Sc2O3/AlGaN/GaN high electron mobility transistors. *physica status solidi (c),* 2**,** 2672-2675.

Kang, B., S. Pearton, J. Chen, F. Ren, J. Johnson, R. Therrien, P. Rajagopal, J. Roberts, E. Piner & K. Linthicum (2006) Electrical detection of deoxyribonucleic acid hybridization with AlGaN/GaN high electron mobility transistors. *APPLIED PHYSICS LETTERS,* 89**,** -.

Kang, B., F. Ren, Y. Heo, L. Tien, D. Norton & S. Pearton (2005b) pH measurements with single ZnO nanorods integrated with a microchannel. *APPLIED PHYSICS LETTERS,* 86**,** -.

Kang, B., F. Ren, L. Wang, C. Lofton, W. Tan, S. Pearton, A. Dabiran, A. Osinsky & P. Chow (2005c) Electrical detection of immobilized proteins with ungated AlGaN/GaN high-electron-mobility transistors. *APPLIED PHYSICS LETTERS,* 87**,** -.

Kang, B., H. Wang, T. Lele, Y. Tseng, F. Ren, S. Pearton, J. Johnson, P. Rajagopal, J. Roberts, E. Piner & K. Linthicum (2007a) Prostate specific antigen detection using AlGaN/GaN high electron mobility transistors. *APPLIED PHYSICS LETTERS,* 91**,** -.

Kang, B., H. Wang, F. Ren, B. Gila, C. Abernathy, S. Pearton, D. Dennis, J. Johnson, P. Rajagopal, J. Roberts, E. Piner & K. Linthicum (2008) Exhaled-breath detection using AlGaN/GaN high electron mobility transistors integrated with a Peltier element. *ELECTROCHEMICAL AND SOLID STATE LETTERS,* 11**,** J19-J21.

Kang, B., H. Wang, F. Ren, S. Pearton, T. Morey, D. Dennis, J. Johnson, P. Rajagopal, J. Roberts, E. Piner & K. Linthicum (2007b) Enzymatic glucose detection using ZnO nanorods on the gate region of AlGaN/GaN high electron mobility transistors. *APPLIED PHYSICS LETTERS,* 91**,** -.

Kang, B. S., S. Kim, F. Ren, B. P. Gila, C. R. Abernathy & S. J. Pearton (2005d) Comparison of MOS and Schottky W/Pt-GaN diodes for hydrogen detection. *Sensors and Actuators B-Chemical,* 104**,** 232-236.

Kang, B. S., H. T. Wang, T. P. Lele, Y. Tseng, F. Ren, S. J. Pearton, J. W. Johnson, P. Rajagopal, J. C. Roberts, E. L. Piner & K. J. Linthicum (2007c) Prostate specific antigen detection using AlGaN/GaN high electron mobility transistors. *Applied Physics Letters,* 91.

Kang, B. S., H. T. Wang, F. Ren, B. P. Gila, C. R. Abernathy, S. J. Pearton, J. W. Johnson, P. Rajagopal, J. C. Roberts, E. L. Piner & K. J. Linthicum (2007d) pH sensor using AlGaN/GaN high electron mobility transistors with Sc2O3 in the gate region. *Applied Physics Letters,* 91.

Kelloff, G. J., D. S. Coffey, B. A. Chabner, A. P. Dicker, K. Z. Guyton, P. D. Nisen, H. R. Soule & A. V. D'Amico (2004) Prostate-specific antigen doubling time as a surrogate marker for evaluation of oncologic drugs to treat prostate cancer. *Clinical Cancer Research,* 10**,** 3927-3933.

Kim, J., B. P. Gila, C. R. Abernathy, G. Y. Chung, F. Ren & S. J. Pearton (2003) Comparison of Pt/GaN and Pt/4H-SiC gas sensors. *Solid-State Electronics,* 47**,** 1487-1490.

Kostikas, K., G. Papatheodorou, K. Ganas, K. Psathakis, P. Panagou & S. Loukides (2002) pH in expired breath condensate of patients with inflammatory airway diseases. *American Journal of Respiratory and Critical Care Medicine,* 165**,** 1364-1370.

Kouassi, G., J. Irudayaraj & G. McCarty (2005) Activity of glucose oxidase functionalized onto magnetic nanoparticles. *Biomagnetic research and technology,* 3**,** 1.

Kouche, A. E. L., J. Lin, M. E. Law, S. Kim, B. S. Kim, F. Ren & S. T. Pearton (2005) Remote sensing system for hydrogen using GaN Schottky diodes. *Sensors and Actuators B-Chemical,* 105**,** 329-333.

Kryliouk, O., H. Park, H. Wang, B. Kang, T. Anderson, F. Ren & S. Pearton (2005) Pt-coated InN nanorods for selective detection of hydrogen at room temperature. *JOURNAL OF VACUUM SCIENCE & TECHNOLOGY B,* 23**,** 1891-1894.

Kullmann, T., I. Barta, E. Csiszer, B. Antus & I. Horvath (2008) Differential Cytokine Pattern in the Exhaled Breath of Patients with Lung Cancer. *Pathology & Oncology Research,* 14**,** 481-483.

Kullmann, T., I. Barta, Z. Lazar, B. Szili, E. Barat, M. Valyon, M. Kollai & I. Horvath (2007) Exhaled breath condensate pH stanclardised for CO2 partial pressure. *European Respiratory Journal,* 29**,** 496-501.

Kumar, S. D., K. Venkatesh & B. Maiti (2004) Determination of chloride in nuclear-grade boron carbide by ion chromatography. *Chromatographia,* 59**,** 243-245.

Langlois, J., W. Rutland-Brown & K. Thomas. 2004. *Traumatic brain injury in the United States: emergency department visits, hospitalizations, and deaths*. Dept. of Health and Human Services, Centers for Disease Control and Prevention, Division of Acute Care, Rehabilitation Research and Disability Prevention, National Center for Injury Prevention and Control.

Lequin, R. M. (2005) Enzyme Immunoassay (EIA)/Enzyme-Linked Immunosorbent Assay (ELISA). *Clinical Chemistry,* 51**,** 2415-2418.

Li, C., M. Curreli, H. Lin, B. Lei, F. N. Ishikawa, R. Datar, R. J. Cote, M. E. Thompson & C. W. Zhou (2005) Complementary detection of prostate-specific antigen using ln(2)O(3) nanowires and carbon nanotubes. *Journal of the American Chemical Society,* 127**,** 12484-12485.

Liehlr, J. G. (2001) Genotoxicity of the steroidal oestrogens oestrone and oestradiol: possible mechanism of uterine and mammary cancer development. *Human Reproduction Update,* 7**,** 273-281.

Lim, W., J. S. Wright, B. P. Gila, J. L. Johnson, A. Ural, T. Anderson, F. Ren & S. J. Pearton (2008) Room temperature hydrogen detection using Pd-coated GaN nanowires. *Applied Physics Letters,* 93.

Lin, C. L., C. L. Shih & L. K. Chau (2007) Amperometric L-Lactate sensor based on sol-gel processing of an enzyme-linked silicon alkoxide. *Analytical Chemistry,* 79**,** 3757-3763.

Lothian, J. R., J. M. Kuo, F. Ren & S. J. Pearton (1992) PLASMA AND WET CHEMICAL ETCHING OF IN0.5GA0.5P. *Journal of Electronic Materials,* 21**,** 441-445.

Lupu, A., A. Valsesia, F. Bretagnol, P. Colpo & F. Rossi (2007) Development of a potentiometric biosensor based on nanostructured surface for lactate determination. *Sensors and Actuators B-Chemical,* 127**,** 606-612.

Luther, B. P., S. D. Wolter & S. E. Mohney (1999) High temperature Pt Schottky diode gas sensors on n-type GaN. *Sensors and Actuators B-Chemical,* 56**,** 164-168.

Machado, R. F., D. Laskowski, O. Deffenderfer, T. Burch, S. Zheng, P. J. Mazzone, T. Mekhail, C. Jennings, J. K. Stoller, J. Pyle, J. Duncan, R. A. Dweik & S. C. Erzurum (2005) Detection of lung cancer by sensor array analyses of exhaled breath. *American Journal of Respiratory and Critical Care Medicine,* 171**,** 1286-1291.

Makimoto, T., Y. Yamauchi & K. Kumakura (2004) High-power characteristics of GaN/InGaN double heterojunction bipolar transistors. *Applied Physics Letters,* 84**,** 1964-1966.

Marquette, C. A., A. Degiuli & L. J. Blum (2000) Fiberoptic biosensors based on chemiluminescent reactions. *Applied Biochemistry and Biotechnology,* 89**,** 107-115.

Matozzo, V., F. Gagne, M. Marin, F. Ricciardi & C. Blaise (2008a) Vitellogenin as a biomarker of exposure to estrogenic compounds in aquatic invertebrates: A review. *ENVIRONMENT INTERNATIONAL,* 34**,** 531-545.

Matozzo, V., F. Gagne, M. G. Marin, F. Ricciardi & C. Blaise (2008b) Vitellogenin as a biomarker of exposure to estrogenic compounds in aquatic invertebrates: A review. *Environment International,* 34**,** 531-545.

McIntyre, R., L. Bigler, T. Dellinger, M. Pfeifer, T. Mannery & C. Streckfus (1999) Oral contraceptive usage and the expression of CA 15-3 and c-erbB-2 in the saliva of healthy women. *Oral Surgery Oral Medicine Oral Pathology Oral Radiology and Endodontics,* 88**,** 687-690.

Mehandru, R., B. Luo, B. Kang, J. Kim, F. Ren, S. Pearton, C. Pan, G. Chen & J. Chyi (2004) AlGaN/GaN HEMT based liquid sensors. *SOLID-STATE ELECTRONICS,* 48**,** 351-353.

Michaelson, J. S., E. Halpern & D. B. Kopans (1999) Breast cancer: Computer simulation method for estimating optimal intervals for screening. *Radiology,* 212**,** 551-560.

Montuschi, P. & P. J. Barnes (2002) Analysis of exhaled breath condensate for monitoring airway inflammation. *Trends in Pharmacological Sciences,* 23**,** 232-237.

Mosconi, G., O. Carnevali, M. F. Franzoni, E. Cottone, I. Lutz, W. Kloas, K. Yamamoto, S. Kikuyama & A. M. Polzonetti-Magni (2002) Environmental Estrogens and reproductive biology in amphibians. *General and Comparative Endocrinology,* 126**,** 125-129.

Namjou, K., C. B. Roller & P. J. McCann (2006) The breathmeter - A new laser device to analyze your health. *Ieee Circuits & Devices,* 22**,** 22-28.

Navarro, M. A., R. Mesia, O. DiezGibert, A. Rueda, B. Ojeda & M. C. Alonso (1997) Epidermal growth factor in plasma and saliva of patients with active breast cancer and breast cancer patients in follow-up compared with healthy women. *Breast Cancer Research and Treatment,* 42**,** 83-86.

Neuberger, R., G. Müller, O. Ambacher & M. Stutzmann (2001) Ion-induced modulation of channel currents in AlGaN/GaN high-electron-mobility transistors. *physica status solidi (a),* 183**,** R10-R12.

Niimi, A., L. T. Nguyen, O. Usmani, B. Mann & K. F. Chung (2004) Reduced pH and chloride levels in exhaled breath condensate of patients with chronic cough. *Thorax,* 59**,** 608-612.

Paige, S. Z. & C. F. Streckfus (2007) Salivary analysis in the diagnosis and treatment of breast cancer: a role for the general dentist. *Gen Dent,* 55**,** 156-7; quiz 158, 167-8.

Pandey, P., S. P. Singh, S. K. Arya, V. Gupta, M. Datta, S. Singh & B. D. Malhotra (2007) Application of thiolated gold nanoparticles for the enhancement of glucose oxidase activity. *Langmuir,* 23**,** 3333-3337.

Park, S., H. Boo & T. D. Chung (2006) Electrochemical non-enzymatic glucose sensors. *Analytica Chimica Acta,* 556**,** 46-57.

Parra, A., E. Casero, L. Vazquez, F. Pariente & E. Lorenzo (2006) Design and characterization of a lactate biosensor based on immobilized lactate oxidase onto gold surfaces. *Analytica Chimica Acta,* 555**,** 308-315.

Patolsky, F., B. Timko, G. Zheng & C. Lieber (2007) Nanowire-based nanoelectronic devices in the life sciences. *MRS BULLETIN,* 32**,** 142-149.

Patolsky, F., G. Zheng & C. Lieber (2006a) Fabrication of silicon nanowire devices for ultrasensitive, label-free, real-time detection of biological and chemical species. *NATURE PROTOCOLS,* 1**,** 1711-1724. (2006b) Nanowire sensors for medicine and the life sciences. *NANOMEDICINE,* 1**,** 51-65.

Pearton, S. J., B. S. Kang, S. K. Kim, F. Ren, B. P. Gila, C. R. Abernathy, J. S. Lin & S. N. G. Chu (2004) GaN-based diodes and transistors for chemical, gas, biological and pressure sensing. *Journal of Physics-Condensed Matter,* 16**,** R961-R994.

Pearton, S. J., T. Lele, Y. Tseng & F. Ren (2007) Penetrating living cells using semiconductor nanowires. *Trends in Biotechnology,* 25**,** 481-482.

Phypers, B. & J. Pierce (2006) Lactate physiology in health and disease. *Continuing Education in Anaesthesia, Critical Care & Pain,* 6**,** 128.

Pohanka, M. & P. Zboril (2008) Amperometric biosensor for D-lactate assay. *Food Technology and Biotechnology,* 46**,** 107-110.

Porte, C., G. Janer, L. Lorusso, M. Ortiz-Zarragoitia, M. Cajaraville, M. Fossi & L. Canesi (2006) Endocrine disruptors in marine organisms: Approaches and perspectives. *COMPARATIVE BIOCHEMISTRY AND PHYSIOLOGY C-TOXICOLOGY & PHARMACOLOGY,* 143**,** 303-315.

Sabo-Attwood, T., J. L. Blum, K. J. Kroll, V. Patel, D. Birkhoiz, N. J. Szabo, S. Z. Fisher, R. McKenna, M. Campbell-Thompson & N. D. Denslow (2007) Distinct expression and activity profiles of largemouth bass (Micropterus salmoides) estrogen receptors in response to estradiol and nonylphenol. *Journal of Molecular Endocrinology,* 39**,** 223-237.

Saito, W., T. Domon, I. Omura, M. Kuraguchi, Y. Takada, K. Tsuda & M. Yamaguchi (2006) Demonstration of 13.56-MHz class-E amplifier using a high-voltage GaN power-HEMT. *Ieee Electron Device Letters,* 27**,** 326-328.

Sandhu, A. (2007) Biosensing - New probes offer much faster results. *Nature Nanotechnology,* 2**,** 746-748.

Schalwig, J., G. Muller, U. Karrer, M. Eickhoff, O. Ambacher, M. Stutzmann, L. Gorgens & G. Dollinger (2002) Hydrogen response mechanism of Pt-GaN Schottky diodes. *Applied Physics Letters,* 80**,** 1222-1224.

Shen, L., R. Coffie, D. Buttari, S. Heikman, A. Chakraborty, A. Chini, S. Keller, S. P. DenBaars & U. K. Mishra (2004) High-power polarization-engineered GaN/AlGaN/GaN HEMTs without surface passivation. *Ieee Electron Device Letters,* 25**,** 7-9.

Spohn, U., D. Narasaiah, L. Gorton & D. Pfeiffer (1996) A bienzyme modified carbon paste electrode for the amperometric detection of L-lactate at low potentials. *Analytica Chimica Acta,* 319**,** 79-90.

Streckfus, C. & L. Bigler (2005) The use of soluble, salivary c-erbB-2 for the detection and post-operative follow-up of breast cancer in women: the results of a five-year translational research study. *Adv Dent Res,* 18**,** 17-24.

Streckfus, C., L. Bigler, T. Dellinger, X. L. Dai, W. J. Cox, A. McArthur, A. Kingman & J. T. Thigpen (2001) Reliability assessment of soluble c-erbB-2 concentrations in the saliva of healthy women and men. *Oral Surgery Oral Medicine Oral Pathology Oral Radiology and Endodontics,* 91**,** 174-179.

Streckfus, C., L. Bigler, T. Dellinger, X. L. Dai, A. Kingman & J. T. Thigpen (2000a) The presence of soluble c-erbB-2 in saliva and serum among women with breast carcinoma: A preliminary study. *Clinical Cancer Research,* 6**,** 2363-2370.

Streckfus, C., L. Bigler, T. Dellinger, M. Pfeifer, A. Rose & J. T. Thigpen (1999) CA 15-3 and c-erbB-2 presence in the saliva of women. *Clin Oral Investig,* 3**,** 138-43.

Streckfus, C., L. Bigler, M. Tucci & J. T. Thigpen (2000b) A preliminary study of CA15-3, c-erbB-2, epidermal growth factor receptor, cathepsin-D, and p53 in saliva among women with breast carcinoma. *Cancer Investigation,* 18**,** 101-109.

Streckfus, C. F., L. R. Bigler & M. Zwick (2006) The use of surface-enhanced laser desorption/ionization time-of-flight mass spectrometry to detect putative breast cancer markers in saliva: a feasibility study. *Journal of Oral Pathology & Medicine,* 35**,** 292-300.

Suman, S., R. Singhal, A. L. Sharma, B. D. Malthotra & C. S. Pundir (2005) Development of a lactate biosensor based on conducting copolymer bound lactate oxidase. *Sensors and Actuators B-Chemical,* 107**,** 768-772.

Sumpter, J. P. & S. Jobling (1995) VITELLOGENESIS AS A BIOMARKER FOR ESTROGENIC CONTAMINATION OF THE AQUATIC ENVIRONMENT. *Environmental Health Perspectives,* 103**,** 173-178.

Taylor, J. S. & S. K. Hong (2000) Potable water quality and membrane technology. *Laboratory Medicine,* 31**,** 563-568.

Thadhani, R., M. Pascual & J. V. Bonventre (1996) Medical progress - Acute renal failure. *New England Journal of Medicine,* 334**,** 1448-1460.

Thompson, I. M. & D. P. Ankerst (2007) Prostate-specific antigen in the early detection of prostate cancer. *Canadian Medical Association Journal,* 176**,** 1853-1858.

Tien, L., P. Sadik, D. Norton, L. Voss, S. Pearton, H. Wang, B. Kang, F. Ren, J. Jun & J. Lin (2005a) Hydrogen sensing at room temperature with Pt-coated ZnO thin films and nanorods. *APPLIED PHYSICS LETTERS,* 87**,** -.

Tien, L., H. Wang, B. Kang, F. Ren, P. Sadik, D. Norton, S. Pearton & J. Lin (2005b) Room-temperature hydrogen-selective sensing using single Pt-coated ZnO nanowires at microwatt power levels. *ELECTROCHEMICAL AND SOLID STATE LETTERS,* 8**,** G230-G232.

Vaidya, V. S. & J. V. Bonventre (2006) Mechanistic biomarkers for cytotoxic acute kidney injury. *Expert Opinion on Drug Metabolism & Toxicology,* 2**,** 697-713.

Vaidya, V. S., V. Ramirez, T. Ichimura, N. A. Bobadilla & J. V. Bonventre (2006) Urinary kidney injury molecule-1: a sensitive quantitative biomarker for early detection of kidney tubular injury. *American Journal of Physiology-Renal Physiology,* 290**,** F517-F529.

Vaughan, J., L. Ngamtrakulpanit, T. N. Pajewski, R. Turner, T. Nguyen, A. Smith, P. Urban, S. Hom, B. Gaston & J. Hunt (2003) Exhaled breath condensate pH is a robust and reproducible assay of airway acidity. *European Respiratory Journal,* 22**,** 889-894.

Verma, R. & R. Parthasarathy (1996) Neutron activation analysis for chlorine in Zr-2.5 wt% Nb coolant tube material. *Journal of Radioanalytical and Nuclear Chemistry,* 214**,** 391-397.

Vignali, D. A. A. (2000) Multiplexed particle-based flow cytometric assays. *Journal of Immunological Methods,* 243**,** 243-255.

Walker, H., W. Hall & J. Hurst. 1990. *Clinical methods: the history, physical and laboratory examinations*. Butterworths Stoneham, MA.

Wang, H., T. Anderson, B. Kang, F. Ren, C. Li, Z. Low, J. Lin, B. Gila, S. Pearton, A. Osinsky & A. Dabiran (2007a) Stable hydrogen sensors from AlGaN/GaN heterostructure diodes with TiB2-based Ohmic contacts. *APPLIED PHYSICS LETTERS,* 90**,** 252109.

Wang, H., T. Anderson, F. Ren, C. Li, Z. Low, J. Lin, B. Gila, S. Pearton, A. Osinsky & A. Dabiran (2006a) Robust detection of hydrogen using differential AlGaN/GaN high electron mobility transistor sensing diodes. *APPLIED PHYSICS LETTERS,* 89**,** -.

Wang, H., B. Kang, T. Chancellor, T. Lele, Y. Tseng, F. Ren, S. Pearton, A. Dabiran, A. Osinsky & P. Chow (2007b) Selective detection of Hg (II) ions from Cu(II) and Pb(II) using AlGaN/GaN high electron mobility transistors. *ELECTROCHEMICAL AND SOLID STATE LETTERS,* 10**,** J150-J153.

Wang, H., B. Kang, F. Ren, R. Fitch, J. Gillespie, N. Moser, G. Jessen, T. Jenkins, R. Dettmer, D. Via, A. Crespo, B. Gila, C. Abernathy & S. Pearton (2005a) Comparison of gate and drain current detection of hydrogen at room temperature with AlGaN/GaN high electron mobility transistors. *APPLIED PHYSICS LETTERS,* 87**,** 172105.

Wang, H., B. Kang, F. Ren, L. Tien, P. Sadik, D. Norton, S. Pearton & J. Lin (2005b) Detection of hydrogen at room temperature with catalyst-coated multiple ZnO nanorods. *APPLIED PHYSICS A-MATERIALS SCIENCE & PROCESSING,* 81**,** 1117-1119.

(2005c) Hydrogen-selective sensing at room temperature with ZnO nanorods. *APPLIED PHYSICS LETTERS,* 86**,** 243503.

Wang, H. T., B. S. Kang, T. F. Chancellor, T. P. Lele, Y. Tseng, F. Ren, S. J. Pearton, W. J. Johnson, P. Rajagopal, J. C. Roberts, E. L. Piner & K. J. Linthicum (2007c) Fast electrical detection of Hg(II) ions with AlGaN/GaN high electron mobility transistors. *Applied Physics Letters,* 91.

Wang, H. T., B. S. Kang, F. Ren, S. J. Pearton, J. W. Johnson, P. Rajagopal, J. C. Roberts, E. L. Piner & K. J. Linthicum (2007d) Electrical detection of kidney injury molecule-1 with AlGaN/GaN high electron mobility transistors. *Applied Physics Letters,* 91.

Wang, J. (2006) Electrochemical biosensors: Towards point-of-care cancer diagnostics. *Biosensors & Bioelectronics,* 21**,** 1887-1892.

Wang, J. X., X. W. Sun, A. Wei, Y. Lei, X. P. Cai, C. M. Li & Z. L. Dong (2006b) Zinc oxide nanocomb biosensor for glucose detection. *Applied Physics Letters,* 88.

Wang, Y., B. Chu, K. Chen, C. Chang, T. Lele, G. Papadi, J. Coleman, B. Sheppard, C. Dungen, S. Pearton, J. Johnson, P. Rajagopal, J. Roberts, E. Piner, K. Linthicum & F. Ren (2009) Fast detection of a protozoan pathogen, Perkinsus marinus, using AlGaN/GaN high electron mobility transistors. *APPLIED PHYSICS LETTERS,* 94**,** -.

Warden, D. Blast Injury. In *Defense and Veterans Brain Injury center*.

Watson, C. S., N. N. Bulayeva, A. L. Wozniak & R. A. Alyea (2007) Xenoestrogens are potent activators of nongenomic estrogenic responses. *Steroids,* 72**,** 124-134.

Wee, K. W., G. Y. Kang, J. Park, J. Y. Kang, D. S. Yoon, J. H. Park & T. S. Kim (2005) Novel electrical detection of label-free disease marker proteins using piezoresistive self-sensing micro-cantilevers. *Biosensors & Bioelectronics,* 20**,** 1932-1938.

Wei, A., X. W. Sun, J. X. Wang, Y. Lei, X. P. Cai, C. M. Li, Z. L. Dong & W. Huang (2006) Enzymatic glucose biosensor based on ZnO nanorod array grown by hydrothermal decomposition. *Applied Physics Letters,* 89.

Wright, J. S., W. Lim, B. P. Gila, S. J. Pearton, F. Ren, W. T. Lai, L. C. Chen, M. S. Hu & K. H. Chen (2009) Pd-catalyzed hydrogen sensing with InN nanobelts. *Journal of Vacuum Science & Technology B,* 27**,** L8-L10.

Yager, J. D. & J. G. Liehr (1996) Molecular mechanisms of estrogen carcinogenesis. *Annual Review of Pharmacology and Toxicology,* 36**,** 203-232.

Yang, Y. H., H. F. Yang, M. H. Yang, Y. L. Liu, G. L. Shen & R. Q. Yu (2004) Amperometric glucose biosensor based on a surface treated nanoporous ZrO2/chitosan composite film as immobilization matrix. *Analytica Chimica Acta,* 525**,** 213-220.

Yu, X., C. Li, Z. N. Low, J. Lin, T. J. Anderson, H. T. Wang, F. Ren, Y. L. Wang, C. Y. Chang, S. J. Pearton, C. H. Hsu, A. Osinsky, A. Dabiran, P. Chow, C. Balaban & J. Painter (2008) Wireless hydrogen sensor network using AlGaN/GaN high electron mobility transistor differential diode sensors. *Sensors and Actuators B-Chemical,* 135**,** 188-194.

Zhang, A. P., L. B. Rowland, E. B. Kaminsky, J. W. Kretchmer, R. A. Beaupre, J. L. Garrett, J. B. Tucker, B. J. Edward, J. Foppes & A. F. Allen (2003) Microwave power SiC MESFETs and GaNHEMTs. *Solid-State Electronics,* 47**,** 821-826.

Zhang, J., H. P. Lang, F. Huber, A. Bietsch, W. Grange, U. Certa, R. McKendry, H. J. Guntgerodt, M. Hegner & C. Gerber (2006) Rapid and label-free nanomechanical detection of biomarker transcripts in human RNA. *Nature Nanotechnology,* 1**,** 214-220.

Zheng, G., F. Patolsky, Y. Cui, W. Wang & C. Lieber (2005a) Multiplexed electrical detection of cancer markers with nanowire sensor arrays. *NATURE BIOTECHNOLOGY,* 23**,** 1294-1301.

Zheng, G. F., F. Patolsky, Y. Cui, W. U. Wang & C. M. Lieber (2005b) Multiplexed electrical detection of cancer markers with nanowire sensor arrays. *Nature Biotechnology,* 23**,** 1294-1301.

Biosensors for Health, Environment and Biosecurity

Edited by Prof. Pier Andrea Serra

ISBN 978-953-307-443-6
Hard cover, 540 pages
Publisher InTech
Published online 19, July, 2011
Published in print edition July, 2011

A biosensor is a detecting device that combines a transducer with a biologically sensitive and selective component. Biosensors can measure compounds present in the environment, chemical processes, food and human body at low cost if compared with traditional analytical techniques. This book covers a wide range of aspects and issues related to biosensor technology, bringing together researchers from 16 different countries. The book consists of 24 chapters written by 76 authors and divided in three sections: Biosensors Technology and Materials, Biosensors for Health and Biosensors for Environment and Biosecurity.

How to reference

In order to correctly reference this scholarly work, feel free to copy and paste the following:

Fan Ren, Stephen J. Pearton, Byoung Sam Kang, and Byung Hwan Chu (2011). AlGaN/GaN High Electron Mobility Transistor Based Sensors for Bio-Applications, Biosensors for Health, Environment and Biosecurity, Prof. Pier Andrea Serra (Ed.), ISBN: 978-953-307-443-6, InTech, Available from: http://www.intechopen.com/books/biosensors-for-health-environment-and-biosecurity/algan-gan-high-electron-mobility-transistor-based-sensors-for-bio-applications

INTECH
open science | open minds

InTech Europe
University Campus STeP Ri
Slavka Krautzeka 83/A
51000 Rijeka, Croatia
Phone: +385 (51) 770 447
Fax: +385 (51) 686 166
www.intechopen.com

InTech China
Unit 405, Office Block, Hotel Equatorial Shanghai
No.65, Yan An Road (West), Shanghai, 200040, China
中国上海市延安西路65号上海国际贵都大饭店办公楼405单元
Phone: +86-21-62489820
Fax: +86-21-62489821

IntechOpen